Winter 12-9-2011

# Generic Strategies to Implement Material Grading in Finite Element Methods for Isotropic and Anisotropic Materials

Ke Yu
*University of Nebraska-Lincoln*, keyuunl@gmail.com

# GENERIC STRATEGIES TO IMPLEMENT MATERIAL GRADING IN FINITE ELEMENT METHODS FOR ISOTROPIC AND ANISOTROPIC MATERIALS

By

Ke Yu

A THESIS

Presented to the Faculty of

The Graduate College at the University of Nebraska

In Partial Fulfillment of Requirements

For the Degree of Master of Science

Major: Engineering Mechanics

Under the supervision of Professor Mehrdad Negahban

Lincoln, Nebraska

Nov, 2011

# GENERIC STRATEGIES TO IMPLEMENT MATERIAL GRADING IN FINITE ELEMENT METHODS FOR ISOTROPIC AND ANISOTROPIC MATERIALS

Ke Yu, M.S.

University of Nebraska, 2011

Advisor: Mehrdad Negahban

We look at generic strategies to transfer material grading into finite element methods. Three strategies are proposed to transfer material grading into the finite element analysis. These strategies are node-centered, element-centered, and the definition of material grading through external functions. The process to achieve each strategy is stated, and examples are used to illustrate each strategy, and to compare them. The strategies are implemented in finite-deformation nonlinear elastic analysis.

Several examples are used to illustrate the implementation of each strategy for graded isotropic materials. For these examples, the results obtained from finite element models are compared with those obtained from classical beam theory to verify the finite element implementation. For graded anisotropic materials, a general finite deformation model for stress is developed and implemented. This model can take account of material grading both in material parameters and direction of the anisotropy. Several examples of graded anisotropic materials are analyzed to verify implementation of the model and compare proposed strategies.

The analysis of the different strategies indicates that when comparing the needed memory, speed, and implementation, new strategies that are based on flexible FEM may provide advantage in solving problems with material grading.

# Acknowledgements

I would like to dedicate this thesis to my mother, sister and brother-in-law for all the support they have been giving to me. Without them, I could not have gone this far.

I would like to thank my professor and mentor, Dr. Mehrdad Negahban, for his guidance and encouragement during the entire process of this thesis. I have no doubt his professional spirit will continue influencing my future life.

I also want to express my thanks to committee members, Dr. Jiashi Yang and Dr. Ruqiang Feng for their time to spend on reading my thesis.

I want to take this opportunity thank all my friends in Lincoln.

Finally, I want to dedicate this thesis to my father. Life is too short to be with the loved ones. Wish him rest in peace.

# Table of Contents

# List of Figures

# List of Tables

# Chapter 1 Introduction

In this thesis I look at finite deformation elastic problems with graded materials and use and compare different strategies of introducing the grading into the finite element method solution.

## 1.1 Introduction to graded materials

In modern applications, traditional homogeneous materials have been giving ways to graded materials due to their higher performance, either in mechanical or thermal properties.

Consider a functionally graded plate (FGM) that is made from grading ceramic and copper through the thickness, and has one ceramics-rich surface and one copper-rich surface. Since these two materials have a large difference in their thermal conductivity, such a ceramics-copper plate that can act as a thermal barrier and yet provide structural strength. The grading allows gradual changes so that the mechanical effect of the huge temperature gradients through the thickness of plate are gradually mitigated, avoiding detrimental stress concentrations. This system can be used in the aerospace industry.

Another example of using graded materials in industry is the use of composites. For example, airplane frames are now mainly made of composites since they can provide equal mechanical performance with less weight, which is quite attractive to airplane manufacturers and airline companies.

Graded materials can be divided into two categories: isotropic and anisotropic materials. The material grading characters for isotropic and anisotropic materials are briefly discussed below.

**Graded isotropic materials:**

Material properties of isotropic materials are independent of direction. As a result, the grading of isotropic materials normally only refers to the scaling of material parameters with respect to positions. The functionally graded ceramic-copper plate described above is an example of graded isotropic materials. In this example, material parameters in the plate vary from the ceramic-rich surface to the metal rich surface.

**Graded Anisotropic materials:**

For anisotropic materials, such as transversely isotropic materials or orthotropic materials, material properties are direction dependent. Therefore, for graded anisotropic materials, both the scaling of material parameters and the orientations of the anisotropy can change.

For example, a laminated composite plate made of orthotropic laminas may have each layer with different material principal orientations. In this case, even without any change of material parameters, this anisotropic material introduces material grading by changing orientations of anisotropy.

## 1.2 FEM in graded materials

The finite element method FEM has played an important role in the design of all kinds of industrial products since its emergence. Researchers and engineers have worked extensively on FEM and developed an efficient system for solving general problems. This section conducts a review of recent literatures on FEM in the graded materials field.

**Functionally graded materials**

For functionally graded materials, the finite element formulation is studied by S. Pradyunma [1], R. Naghadabadi[2], G. N. Praveen and J. N. Reddy [3], J. N. Reddy[5], L. D. Croce [7], Ki-Du Kim[8].

Among these, geometrically nonlinear responses of functionally graded curved panels are analyzed by S. Pradyunma et al. [1]. This study used higher order $C^0$ shell element with nine degrees of freedom at each node, and parabolic transverse shear strain distribution is assumed.

R. Naghadabadi et al. [2] formulated a finite element containing the analytical through-the-thickness integration inherently. Without using Gauss points in the thickness direction, the formulation accounted for the large gradient of the material properties.

G. N. Praveen and J.N. Reddy [3] investigated functionally graded ceramic-metal plate responses under both static and dynamic conditions by using a plate element, which considered transverse shear strains, rotary inertia and moderately large rotations.

L. D. Croce et al. [7] constructed a framework of FEM to analyze functionally graded materials and assessed the convergence, stability and shear locking properties of the formulation.

Ki-Du Kim et al. [8] used a four-node shell element to investigate geometrical nonlinear behavior of FGM structures. The results obtained from the FEM based on first-order shear deformation theory and from numerical analysis are compared.

In these papers, the general form to determine stresses is $\boldsymbol{\sigma} = Q\boldsymbol{\varepsilon}$, in which $\boldsymbol{\sigma}$ is stress vector, $Q$ is stiffness coefficient matrix and $\boldsymbol{\varepsilon}$ is the strain vector. By defining stiffness coefficient matrix to depend on position, material grading of FGMs is handled in finite element formulations.

**Composites:**

M. Braun et al. [9] used 7-parameter shell formulation to simulate the response of laminated structures with arbitrary large displacements and rotations. Transverse normal strain is allowed to vary linearly along the thickness of laminas by using the 7-parameter formulation.

A tensor-based finite element formulation was developed in R. A. Arciniega, J. N. Reddy [10]. A first-order shell theory with seven parameters was derived with exact nonlinear deformations and under the framework of the Lagrangian description.

Based on third order shear deformation theory, a geometrically isoparametric shell element was developed in Mohamed Balah, Hamdan N. Al-Ghamedy [11]. The developed element has seven degrees of freedom per node. A natural strain method [12] was adopted to avoid shear locking.

Sanders Nonliear shell kinematics [14-17] and the third-order shell theory [17, 18] are used to develop a finite element model to study the deflection control of laminated shells in S. J. Lee, J. N. Reddy, F. Rostam-Abadi [13].

L. Vu-Quoc, X. G. Tan [19] developed a simple low-order solid-shell element formulation, in which the element only has displacement-degrees of freedom. Shear locking and curvature thickness locking were avoided by using the assumed natural strain method (ANS).

Many papers focus on finite element formulations to deal with material grading. However, to the best of the author's knowledge, few literatures studied generic strategies to directly transfer material grading into finite elements, without changing traditional finite element formulations. The practical strategies to transfer material grading are studied here, in order to

avoid developing new FE formulations. And a general finite deformation model for stress is developed and implemented in this thesis.

## 1.3 Introduction to nonlinear elasticity

The following contains a review of continuum mechanics and finite deformation elasticity.

### 1.3.1 Kinematics

Displacement **u** of a particle is the vector given by

$$\boldsymbol{u} = \boldsymbol{x} - \boldsymbol{X}, \tag{1.1}$$

where $\boldsymbol{x}$ and $\boldsymbol{X}$ stand for current position and initial position, respectively, of an arbitrary particle.

The deformation gradient is a second-order tensor that contains the information needed to calculate the strain of a small neighborhood around a particle. The deformation gradient $\boldsymbol{F}$ is the partial derivative of the current position with respect to initial position of a particle given by

$$\boldsymbol{F} = \boldsymbol{grad}(\boldsymbol{x}). \tag{1.2}$$

This gives

$$d\boldsymbol{x} = \boldsymbol{F}d\boldsymbol{X}. \tag{1.3}$$

Similarly, the displacement gradient $\boldsymbol{H}$ is defined as

$$\boldsymbol{H} = \boldsymbol{grad}(\boldsymbol{u}) = \boldsymbol{F} - \boldsymbol{I}. \tag{1.4}$$

And this gives

$$d\boldsymbol{u} = \boldsymbol{H}d\boldsymbol{X}. \tag{1.5}$$

The time derivative of a scalar function of the deformation gradient is equal to the scalar product between the partial derivative of that scalar with respect to the deformation gradient and the derivative of deformation gradient with respect to time, and written as

$$\dot{I} = \partial_{\boldsymbol{F}}(I) : \dot{\boldsymbol{F}}. \tag{1.6}$$

For example, if given $I = tr(\boldsymbol{C})$,

$$\dot{I} = \overline{\dot{tr}(\boldsymbol{F}^T\boldsymbol{F})} = tr\left(\dot{\boldsymbol{F}}^T\boldsymbol{F}+\boldsymbol{F}^T\dot{\boldsymbol{F}}\right) = tr\left(\dot{\boldsymbol{F}}^T\boldsymbol{F}\right)+tr\left(\boldsymbol{F}^T\dot{\boldsymbol{F}}\right) = 2\boldsymbol{F} : \dot{\boldsymbol{F}}. \tag{1.7}$$

Therefore, $\partial_{\boldsymbol{F}}(I) = 2\boldsymbol{F}$.

### 1.3.2 Cauchy stress, nominal stress, and tangent modulus

The Helmholtz free energy ψ expresses strain energy per unit mass. For an elastic material, the Cauchy stress tensor $\boldsymbol{T}$ can be calculated by taking the derivative of the specific free energy ψ with respect to the deformation gradient through the relation

$$\boldsymbol{T} = \rho\partial_{\boldsymbol{F}}(\psi)\boldsymbol{F}^T, \tag{1.8}$$

where $\rho$ is the current mass density.

The nominal stress tensor $\boldsymbol{T}_O$ can be calculated from Cauchy stress from the relation

$$\boldsymbol{T}_O = det(\boldsymbol{F})\boldsymbol{F}^{-1}\boldsymbol{T}. \tag{1.9}$$

The tangent modulus of the nominal stress [24], denoted by $\boldsymbol{E}$, is needed to construct the element stiffness arrays in the FEM formulation. It is defined as the partial derivative of the transpose of nominal stress with respect to deformation gradient:

$$\boldsymbol{E} = \partial_{\boldsymbol{F}}(\boldsymbol{T}_o^T). \tag{1.10}$$

## 1.4 Finite element formulations

In this thesis, both brick and shell elements are considered. The shell formulation is an extended-Reissner/Mindlin shell element developed in Negahban [24] to provide geometrically exact nonlinearity of shell structures that uses full thickness integration.

In the shell formulation, the "B-array" is defined as the incremental change of the components of the displacement gradient $\boldsymbol{H}$ with respect to nodal unknowns. This relation is

$$B_{mnqj} = \frac{\partial H_{mn}}{\partial U_{qj}}, \tag{1.11}$$

where $H_{mn}$ are the components of the displacement gradient, and $U_{qj}$ is the unknown $j$ of element node $q$. In this equation, m and n represent indices from 1 to 3, $q$ represents nodes from the first to the last in an element, and $j$ represents degrees of freedom, index $j$ goes from 1 to 3 in brick elements and from 1 to $6 + n_t$, where $n_t$ are the thickness degrees of freedom. It should be pointed out that "B-array" in other paper is the form of matrix, combining the first and last two indices.

Element load and stiffness arrays can be calculated respectively from two equations:

$$F_{pi}^{e} = -\int_{-1}^{1}\int_{S_{iso}} B_{klpi} T_{olk} J_o \, dS_{iso} \, d\xi_3, \qquad 1.12$$

and $$K_{piqj}^{e} = \int_{-1}^{1}\int_{S_{iso}} B_{klpi} E_{klmn} B_{mnqj} J_o \, dS_{iso} \, d\xi_3, \qquad 1.13$$

where $F_{pi}^{e}$ and $K_{piqj}^{e}$ are, respectively, the load and stiffness arrays of elements, $p$ and q are indices to represent nodes in the element, i and j are indices to represent the degrees of freedom for each node, $J_o = det(\boldsymbol{J_o})$, $\boldsymbol{J_o}$ is Jacobian tensor in the initial configuration, $S_{iso}$ is the area of the isoparametric surface element, $\xi_3$ is a curvilinear coordinate from -1 to 1 and along director of the shell, $B_{klpi}$ is "B-array", $T_{olk}$ and $E_{klmn}$ are, respectively, the components of $\boldsymbol{T}_0$ and tangent modulus $\boldsymbol{E}$, k, l, m, n are indices from 1 to 3. The two pairs of indices, *p*-*i* and *q*-*j*, correspond to the two indices of the element stiffness matrix $K_{ab}^{e}$ in other papers.

In this study, the nominal stress and tangent modulus are position dependent due to the material grading, and are given as $\boldsymbol{T}_0(\boldsymbol{F}, \boldsymbol{X})$, and $\boldsymbol{E}(\boldsymbol{F}, \boldsymbol{X})$. By defining the dependence of these factors on $\boldsymbol{X}$, the material grading can be transferred to the FEM model. This will be detailed in Chapter 2.

### 1.4.1 FEMSolid FE package

The FEMSolid finite element package, which was originally developed by Dr. Negahban, is used in this thesis for the finite element analysis. The displacement, strain and stress can be obtained through the solver of FEMSolid. As in figure 1.1 below, the time to assemble and solve the finite element model is shown, so are displacements for each node. The deformed shape of a shell structure is also shown in the figure 1.2.

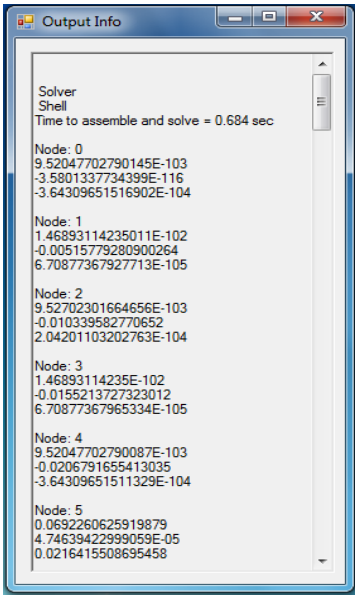


Figure 1.1: Output information of FEMSolid package

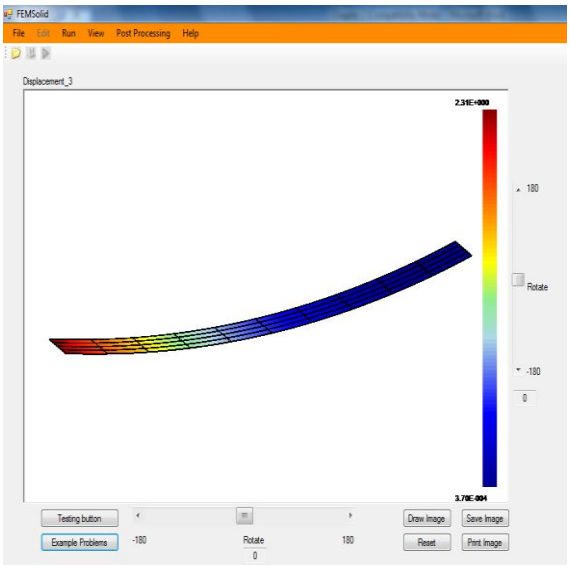


Figure 1.2 Deformation view of finite element model

## 1.5 Objectives and outline of thesis

### 1.5.1 Objectives of thesis

Researchers have worked extensively on finite element formulations to deal with material grading. The objective of this thesis is to develop generic strategies to transfer material grading into the finite element method in order to avoid developing new finite element formulations.

Tensor-based and large deformation constitutive models are not widely used in FEM of graded materials. Therefore, a general finite deformation stress model is proposed in this thesis.

The generic strategies proposed in this thesis will be applicable for both isotropic and anisotropic graded materials.

### 1.5.2 Outline of thesis

Chapter 2 introduces three strategies to transfer material property variations into finite element. These are the global node driven strategy, the element driven strategy, and the function driven strategy. The philosophy and method to achieve each strategy are detailed here.

Chapter 3 provides verifications of the strategies proposed in Chapter 2 through several examples. Comparisons are made among strategies and the traditional finite element method.

Chapter 4 develops a constitutive model to deal with material grading in isotropic and anisotropic materials. Two examples are used to verify the constitutive model.

Chapter 5 uses strategies and constitutive model to study linear and nonlinear of several graded problems.

Conclusions are drawn in Chapter 6 based on previous chapters.

The appendix includes the calculation of the results from classical beam theory. Those results are used as comparison to the results obtained from the FEM implementations.

# Chapter 2 Generic strategies to transfer material grading to finite element model

In this chapter I look at the finite element method implementation for graded materials. Three strategies are proposed to introduce material grading into the finite element modeling. After describing the philosophy behind each strategy, examples are used to illustrate the method.

## 2.1 Finite element implementation for graded materials

### 2.1.1 Stress and tangent modulus for graded materials

For homogeneous materials the Cauchy stress $\boldsymbol{T}$, nominal stress $\boldsymbol{T}_0$, and tangent modulus of stress $\boldsymbol{E}$ are only related to deformation gradient $\boldsymbol{F}$ (or strains $\boldsymbol{\epsilon}$) and can be expressed as functions of the form $\boldsymbol{T}(\boldsymbol{F})$, $\boldsymbol{T}_0(\boldsymbol{F})$ and $\boldsymbol{E}(\boldsymbol{F})$. However, for graded materials the properties change with respect to position. Therefore, for graded materials the Cauchy stress, nominal stress, and tangent modulus depend both on the deformation gradient and the position, and can be expressed as functions of the form $\boldsymbol{T}(\boldsymbol{F},\boldsymbol{X})$, $\boldsymbol{T}_0(\boldsymbol{F},\boldsymbol{X})$ and $\boldsymbol{E}(\boldsymbol{F},\boldsymbol{X})$.

For example, the constitutive model used to describe an isotropic elastic material in this work is characterized by the infinitesimal shear modulus $G$ and bulk modulus $\kappa$, and for graded bodies these two material parameters are assumed to be functions of position. We can write this model as

$$\boldsymbol{T} = \frac{k(\boldsymbol{X})log(J)}{J}\boldsymbol{I} + \frac{G(\boldsymbol{X})}{J^{\frac{5}{3}}}(\boldsymbol{F}\boldsymbol{F}^T - \frac{tr(\boldsymbol{F}\boldsymbol{F}^T)}{3}\boldsymbol{I}), \tag{2.1}$$

$$\boldsymbol{T}_o = k(\boldsymbol{X})log(J)\boldsymbol{F}^{-1} + \frac{G(\boldsymbol{X})}{J^{\frac{2}{3}}}(\boldsymbol{F}^T - \frac{tr(\boldsymbol{F}\boldsymbol{F}^T)}{3}\boldsymbol{F}^{-1}). \quad (2.2)$$

For this case the tangent modulus of the nominal stress is calculated from $\boldsymbol{E} = \partial_{\boldsymbol{F}}(\boldsymbol{T}_o)$ and given by

$$E_{ijmn} = \kappa(\boldsymbol{X})F_{ij}^{-1}F_{nm}^{-1} - \frac{2G(\boldsymbol{X})}{3J^{\frac{2}{3}}}\left(F_{ji}F_{nm}^{-1} - \frac{tr(FF^T)}{3}F_{ij}^{-1}F_{nm}^{-1}\right) - \frac{2G(\boldsymbol{X})}{3J^{\frac{2}{3}}}F_{mn}F_{ij}^{-1} + \frac{G(\boldsymbol{X})}{J^{\frac{2}{3}}}\delta_{in}\delta_{jm} +$$

$$\frac{G(\boldsymbol{X})tr(FF^T)}{3J^{\frac{2}{3}}}F_{im}^{-1}F_{nj}^{-1} - \kappa(\boldsymbol{X})log(J)F_{im}^{-1}F_{nj}^{-1}, \quad (2.3)$$

where $E_{ijmn}$ is the components of the tangent modulus of the nominal stress.

### 2.1.2 Finite element formulation for graded materials

As introduced in section 1.3.4, the element stiffness and load arrays are given

$$F_{pi}^e = -\int_{-1}^{1}\int_{S_{iso}} B_{klpi}T_{olk}J_o dS_{iso}d\xi_3, \quad (2.4)$$

and

$$K_{piqj}^e = \int_{-1}^{1}\int_{S_{iso}} B_{klpi}E_{klmn}B_{mnqj}J_o dS_{iso}d\xi_3. \quad (2.5)$$

These integrals can be calculated by Gaussian Quadrature that calculates weighted summation of the integrand values at specified integration points.

In the nonlinear FEM, the nominal stress and tangent modulus at each integration point is needed to calculate integrals. As discussed in section 2.2.1, the nominal stress and tangent modulus are position dependent for graded materials. Therefore, we need to both describe the variation of material properties in the finite element model, and use this to evaluate the correct properties at each integration point to calculate the nominal stress and tangent modulus.

### 2.1.3 Finite element model

As shown in flow chart of a typical FEM solver given in Figure 2.1, the FEM process start with an FEM model that describes the geometry of the problem using nodes and elements. Next, using the constitutive model and dead loads the element stiffness and load arrays are calculated and assembled into the global stiffness and load arrays. Then, boundary conditions are introduced into the global arrays and the system is given to the FEM solver to calculate a linear FE solution. The solution is then tested for convergence. If the solution has not converged to a stable solution, the unknowns are incremented and the solution process is started again. This process is repeated until the solution converges.

In the classical FE setup the material properties in each element are constant, and more frequently the properties are constant over segments of the body. As a result, the classical FE setup has a way to capture graded properties which is through using many elements, each having different properties. We will consider this the base setup and use it to compare the three following strategies, each of which uses a different strategy to introduce the grading into each element.

Several strategies can be taken to transfer material grading into the element so that the integration points can have different associated properties. One method is to add material grading information onto the components that define the geometry in the FE model. This could be done either through adding the property information to each node or element. Material grading can also be defined outside the FE model. In this case one defines functions for the grading and each integration point obtains its material properties by visiting the functions. This chapter introduces these three strategies and how they get implemented in the FE analysis.

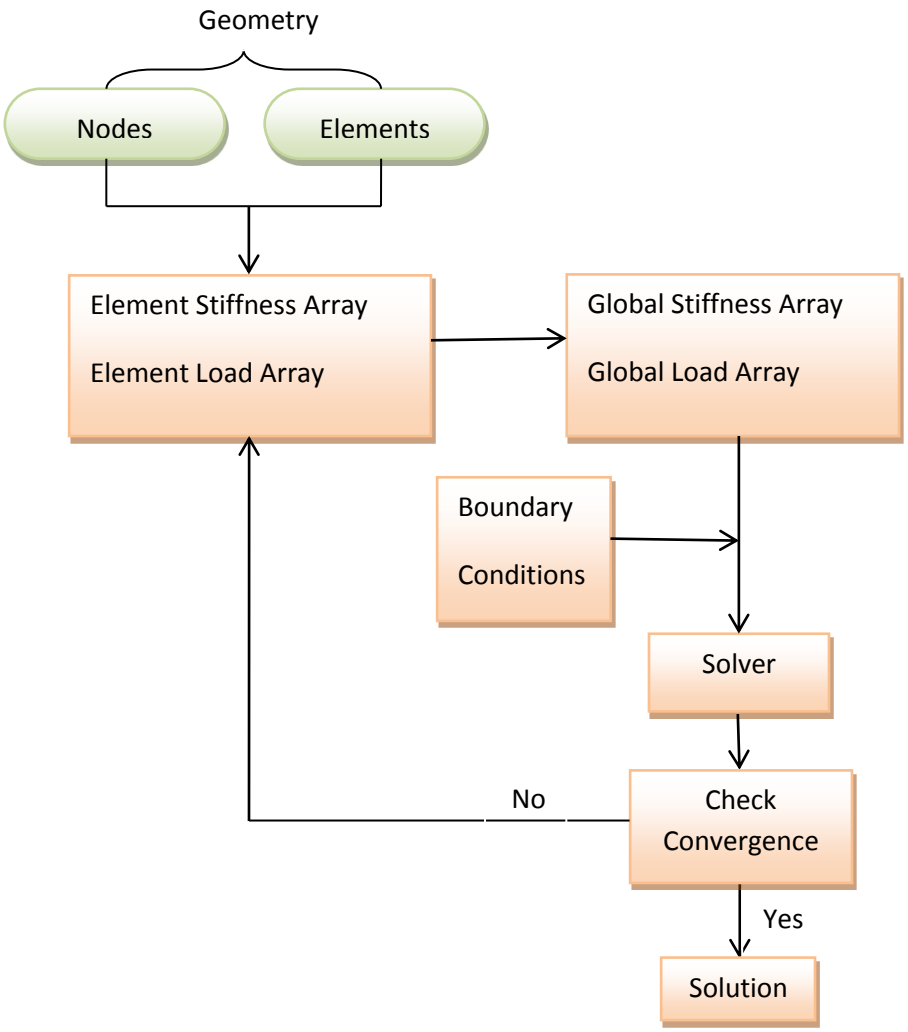


Figure 2.1: Flow chart of FE analysis

## 2.2 Generic strategies to transfer material grading to the FEA

We propose three strategies to transfer material grading into the finite element analysis. These three strategies include adding properties to each global node, to add information about the distributions to each element, and to externally define functions for the distributions. These re respectively called the global node driven strategy, the element driven strategy, and the function driven strategy.

## 2.2.1 Global node driven strategy

### Philosophy of global node driven strategy

In the global node driven strategy, every node within the finite element model is assigned its own material properties. The elements then obtain the material properties at each integration point through interpolation of the node properties.

### Example to illustrate global node driven strategy

Example 1: The first example is of a graded isotropic plate that has a length of 10 inch, width of 2 inch, and thickness of 1 inch, as shown in the Figure 2.2. The elastic modulus is assumed to be 800 psi at its left end and 1200 psi at its right end, and linearly increasing from 800 psi to 1200 along the length of the plate. The Poisson's ratio is assumed to be 0.3 and constant through the entire body. The coordinate system is set up as shown in the figure. Letting $E$ and ν respectively denote the elastic modulus and Poisson's ratio, we will have $E = 800\ (1 + 0.05\ x_1)$, and $\nu = 0.3$.

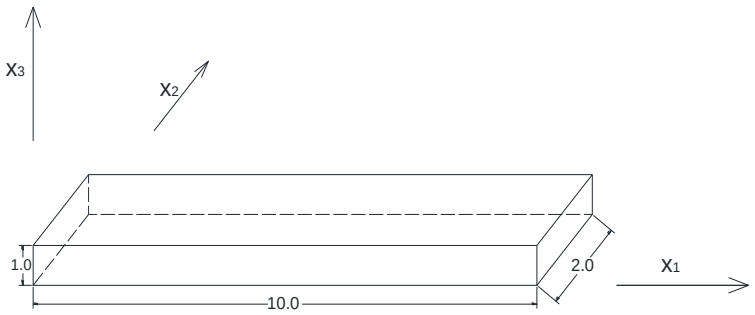


Figure 2.2: Dimensions and coordinates of graded isotropic plate for example 1

The plate is meshed into two four-node elements. Each node in the FEA is given a unique global node number, as shown in Figure 2.3.

For this strategy we need to calculate the properties of the material at each node. For example, node 3 has coordinates $x_1 = 5.0, x_2 = 0.0$ and $x_3 = 0.5$. We thus get for node 3 the properties $E = 800\,(1 + 0.05\,x_1) = 1000$ psi, and $\nu = 0.3$. Following the same method, material properties at all nodes can be calculated to get modulus and Poisson's ratio for each node to be given as: 1(800, 0.3), 2(800, 0.3), 3(1000, 0.3), 4(1000, 0.3), 5(1200, 0.3), 6(1200, 0.3).

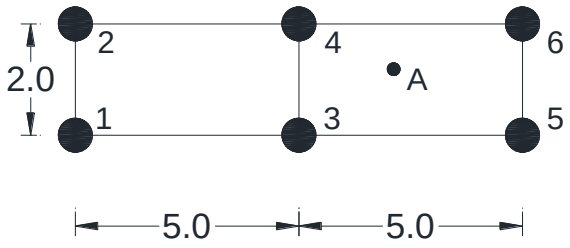


Figure 2.3: Elements and global nodes assignments in FE model for example 1

Once the properties at each node are known, the properties at every point in an element are calculated by interpolating using the properties at the nodes of the element. For example, point A is locates in element 2, which is constructed from node 3, 4, 5, and 6 so its material properties can be obtained by interpolating between the properties of node 3, 4, 5 and 6. Assume point A has coordinate $X$, we can use the shape functions of the element to calculate the properties as

$$E_A = \sum N_i(X) E_i, \tag{2.6}$$

and

$$\nu_A = \sum N_i(X) \nu_i, \tag{2.7}$$

where $i = 3, 4, 5, 6$, $N_i$ are interpolation (shape) functions, $E_i$ and $\nu_i$ are, respectively, the elastic modulus and Poisson's ratio of node $i$.

In this strategy material grading is transferred to the integration points through the properties at the global node and the interpolations in the elements. We thus call this a global node driven strategy.

### 2.2.2 Element driven strategy

In the element driven strategy we assign the distribution of properties in each element. In particular, in the strategy we have followed we assign a property in the element for each node assigned to the element. This allows nodes that are shared by different elements to have assigned to them different properties by different elements. We use the concept of local node numbers to organize the properties in each element.

**Local nodes numbers:**

Node numbering divided into global node numbers and local node numbers. Global node numbers are assigned on entire FE model, and each global node number is unique. Local node numbers are assigned within an element. As shown in Figure 2.4, the global node numbers are node 1 to 6 and span two elements of the FE model, while local node numbers go from 1 to 4 in each element.

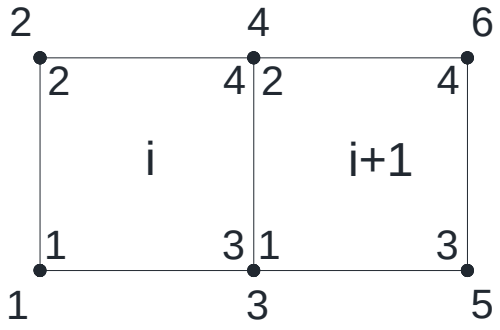


Figure 2.4: Element and node assignment for example 2

**Philosophy of the element driven strategy**

In the element driven strategy, material grading is stored in the elements defining the geometry of FE model. For each node of an element, we store its properties in the element and use the interpolation in the element to calculate the properties at each point in the element.

**Example to illustrate element driven strategy**

Example 2: The second example we consider is of a graded isotropic plate that has thickness of 1.0 inch, width of 2.0 inch, and length 12.0 inch, coordinates x, y, and z along, respectively, the length, width, and thickness, as shown in the Figure 2.5. Along the length, this plate is evenly divided into two parts with the left part, denoted as A, having an elastic modulus of 2000 psi, and the right part, denoted as B, having the elastic modulus of 500 psi. The Poisson's ratio is assumed to be constant through the entire body, and equal to 0.3. Using $E$ and ν to denote the elastic modulus and Poisson's ratio, we can define the properties as

$$E(x) = \begin{cases} 2000, & x < 6 \\ 500, & x \geq 6' \end{cases} \qquad 2.8$$

and

$$\nu = 0.3. \qquad 2.9$$

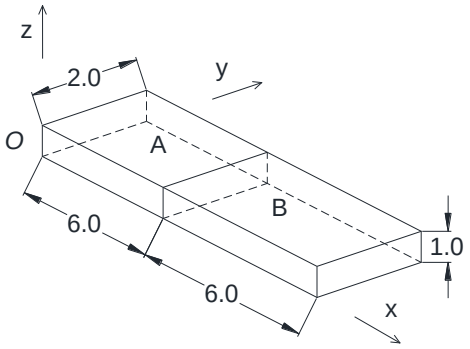


Figure 2.5: Dimensions and coordinates of graded isotropic material

For this example the plate is meshed into two four-node elements. Each local node in the FE model is assigned with a local node number for identification as shown in Figure 2.6. Element 1 is in the region $x < 6$, therefore the nodes in Element 1 are assigned material properties $E = 2000$ psi, $\nu = 0.3$. Element 2 is in the region $x \geq 6$, therefore the nodes in Element 2 are assigned material properties $E = 500$ psi, $\nu = 0.3$.

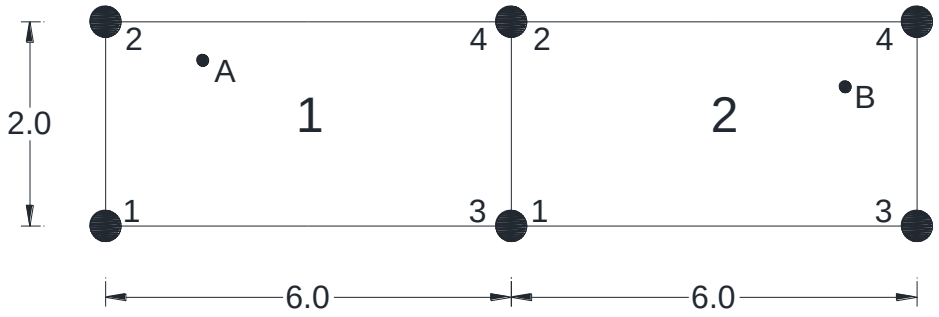


Figure 2.6: Shell elements and local nodes assignments for example 2

Point A is located in element 1, material properties of point A can be obtained by interpolating material properties of local nodes 1, 2, 3 and 4 in element 1. Similarly, material properties of point B can be obtained by interpolating material properties of local nodes 1, 2, 3 and 4 in element 2. Assume point A has coordinate $X_A$ and point B has coordinate $X_B$, the elastic moduli of these two points can be obtained by relations

$$E_A = \sum N_j(X_A) E_{1j}, \tag{2.10}$$

and

$$E_B = \sum N_j(X_B) E_{2j}, \tag{2.11}$$

where $E_{ij}$ denotes the elastic modulus on local node $j$ of element $i$, $i = 1, 2$, $j = 1, 2, 3, 4$, and $N_j$ are interpolation functions for the associated elements.

For this strategy the material grading is transferred to the point in the element through the stored properties in the element and, therefore the, the method is termed the element driven strategy.

For the global node driven strategy and the element driven strategy, material grading is transferred to finite element by interpolating material properties of nodes, properties that are either stored in the global nodes, or in the element and assigned to the local nodes. In the following we consider a totally different strategy.

### 2.2.3 Function driven strategy

**Philosophy of function driven strategy**

For the function driven strategy the material grading is expressed in externally defined functions. While calculating the element stiffness and load arrays, the FE program goes to every integration point and calculates the stress and tangent modulus. In the process, at each integration point the FE program goes to the function and obtains the properties given the points location. This is different from the previous two strategies since the material grading is not assigned to FE nodes or element. Therefore, the FE model does not need to keep the information of material grading inside itself, it just gets material grading by visiting the functions defining it.

**Examples to illustrate the function driven strategy**

**Example 1:** In example 1, the material grading was expressed in the form of functions $E = 800\ (1 + 0.05\ x_1)$, and $\nu = 0.3$. Elements and nodes of the FE model are shown in Figure 2.7. Point A in the figure has coordinates $x_1 = 0.8$, $x_2 = 1.2$, and $x_3 = 0.2$, and point B has coordinates $x_1 = 7.0$, $x_2 = 0.8$, and $x_3 = 0$.

Through the link between the finite element and functions, the finite element can visit the functions $E = 800\ (1 + 0.05\ x_1)$, and $\nu = 0.3$. As a result, the material properties on point A can be directly calculated as $E = 800\ (1 + 0.05\ x_1) = 830$ psi, and $\nu = 0.3$, and that of point B as $E = 800\ (1 + 0.05\ x_1) = 1080$ psi, and $\nu = 0.3$. Hence, material grading is introduced directly through the function.

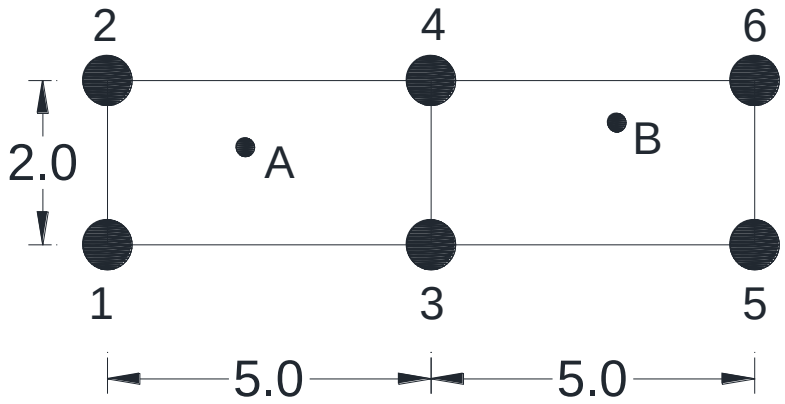


Figure 2.7: Element and node assignment for example 1

**Example 2**: We consider example 2 again, and take A to have coordinates $x_1 = 5.2$, $x_2 = 1.4$, and $x_3 = 0.15$, and point B to have coordinates $x_1 = 7.0$, $x_2 = 0.8$, and $x_3 = 0$.

Through the link between the finite element solver and the functions, FE solver can visit the functions

$$E = \begin{cases} 2000, & x < 6 \\ 500, & x > 6' \end{cases} \tag{2.12}$$

and $$\nu = 0.3. \tag{2.13}$$

Therefore, the material properties for point A can be calculated as $E = 2000$ psi, and $\nu = 0.3$, and for point B as $E = 500$ psi, and $\nu = 0.3$.

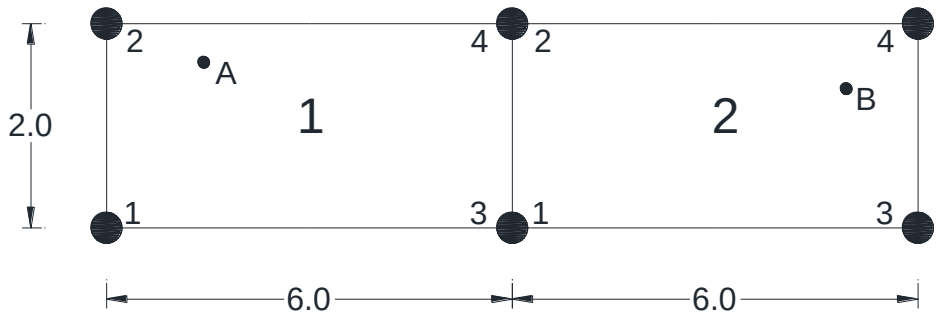


Figure 2.8: Elements and local nodes assignment for example 2

## 2.3 Conclusion

In this chapter the finite element implementation for graded materials is described. Due to the material grading, the stresses and tangent modulus become position dependent. The stresses and tangent modulus for graded isotropic materials are provided as an example to illustrate the position dependence of the properties. In the finite element formulation, the stress and tangent modulus at the integration points are needed in the calculation of the element stiffness and load arrays. To correctly calculate these, material grading must be stored and used at each integration point. According to FE setup, material grading can be added as properties stored in the node, elements, or externally (separately) defined from the FE model.

Three strategies are proposed to introduce material grading into the finite element implementation. These are termed the global node driven strategy, the element driven strategy, and the function driven strategy. For the global node driven strategy, material properties are assigned to each global node. In this case integration points can calculate their properties by interpolating those of the global nodes in the same element. For the element driven strategy, material grading is stored in the element. By interpolating material properties between the properties of the local nodes in the same element, integration points can calculate their

properties. For the function driven strategy, material properties of integration points are obtained directly by visiting material grading functions outside of the FE model. These strategies were illustrated by examples.

# Chapter 3 Verifications and comparisons of strategies

In this chapter, three examples are used to verify and compare the three strategies proposed in Chapter 2. These examples are, respectively, a cantilever with constant material properties, a cantilever with gradual material grading along its length, and a cantilever with a material property jump along its length.

All three strategies are used in each example and compared to the results obtained from beam theory to verify the implementation of each strategy.

Traditional finite element method assigns constant material properties to each element, so that material grading can only be introduced by using many elements each having small property jumps with adjacent elements. To compare the advantages of each strategy and traditional FEM in situations of material grading, a traditional finite element analysis is also done for each example and considered as the base FEA in the following results.

In the comparisons we considered convergence rates, result accuracy, and memory usage of each strategy compared to the base FEA.

**Introduction to Meshing**

Here we consider structure used to mesh the examples. We use both *h* and *p* methods to increase the accuracy and convergence rate. The *h*-method uses more elements, and the *p*-method uses higher order elements to achieve this goal. As shown in the Figure 3.1, the number of nodes along length and width directions are, respectively, denoted $m$ and $n$ for shell elements and expressed as an $m \times n$ element. The *p*-method will essentially increase the *m* or *n* in the examples. As shown in the Figure 3.2, the numbers of elements along length and width

directions are, respectively, given by $M$ and $N$, and the number of elements in a shell is denoted by the expression $M \times N$. The *h*-method will increase the *M* and *N* in the example.

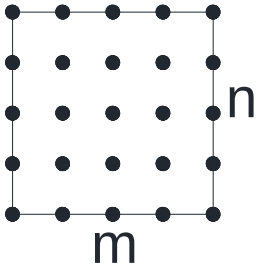


Figure 3.1: m × n nodes in an element

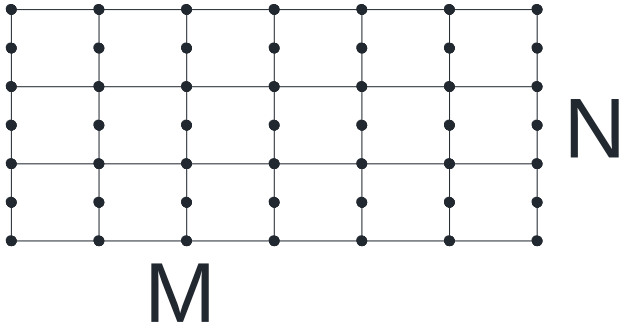


Figure 3.2: M × N elements in FE model

## 3.1 Description of examples

### 3.1.1 Example 1: Cantilever with constant material properties

The first example is a uniform cantilever that is loaded with a vertical force at its free end as shown in Figure 3.3. This example has material constant material properties and can be considered a non-graded example used for verification of the implementation. The cantilever has a width of 1 inch, a height of 1 inch, and a length of 10 inch, and with a uniform elastic modulus $E$ = 1600 psi, and Poisson's ratio $\nu = 0.3$. The shear modulus $G$ and bulk modulus $\kappa$ can be obtained by the standard relations: $G = \frac{E}{2(1+\nu)}$, and $\kappa = \frac{E}{3(1-2\nu)}$.

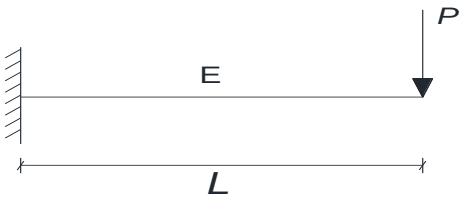


Figure 3.3: Diagram of cantilever with constant material properties

### 3.1.2 Example 2: Cantilever with linear grading of properties along the length

In this example the material properties are assumed to linearly vary along length of a cantilever. The loading is the same as the previous example. Figure 3.4 shows the loading on the cantilever, the variation of the elastic modulus, and bending moment in the cantilever. The cantilever has a thickness of 1 inch, a width of 1 inch, and a length of 10 inch. The elastic modulus is 1200 psi at its fixed end and linearly decreases to 800 psi at its free end. This gives an equation for the elastic modulus as $E(x) = 800\ (1 + 0.05\ x)$. The Poisson's ratio is taken as uniform and given by $\nu = 0.3$.

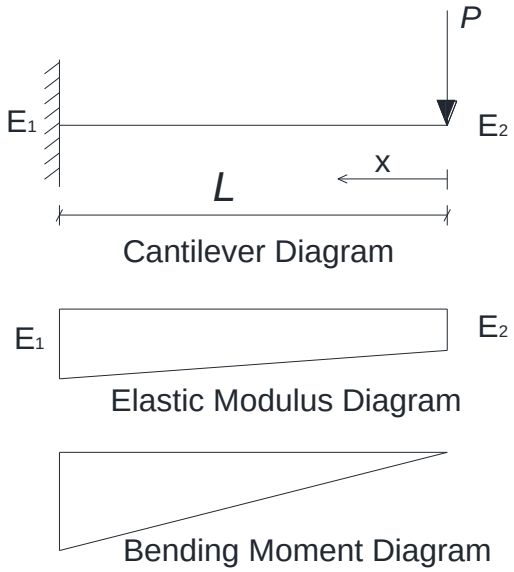


Figure 3.4: Diagrams of cantilever, elastic modulus, and bending moment

### 3.1.3 Example 3: Cantilever with a jump in properties along the length

In this example, as shown in Figure 3.5, the cantilever is composed of two parts A and B that are made from different uniform materials. As a result, the material properties undergo an abrupt change on the boundary between these two parts, but remain constant within each part. The cantilever has a thickness of 1 inch, a width of 1 inch, and a length of 12 inch. The material of part A has an elastic modulus 2000 psi, and the material of part B has an elastic modulus 500 psi. The Poisson's ratio for both parts is taken as $\nu = 0.3$. Figure 3.6 shows the variation of the elastic modulus and bending moment in the cantilever.

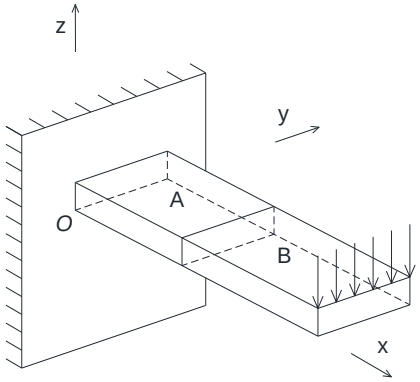


Figure 3.5: Cantilever diagram

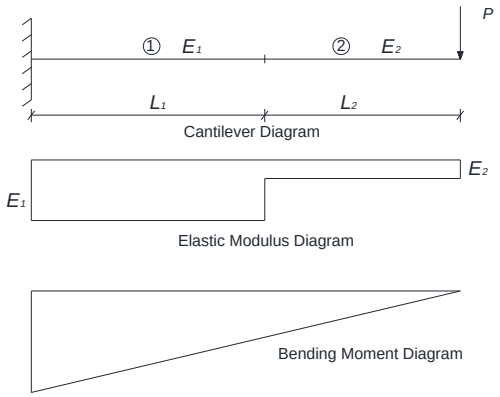


Figure 3.6: Diagrams of cantilever, elastic modulus and bending moment

## 3.2 Verifications of implementation of strategies

### 3.2.1 Verifications using uniform cantilever (Example 1)

Example 1 introduced in section 3.1.1 is a non-graded cantilever used here to verify the implementation. The results obtained from beam theory are provided as reference to compare the results obtained from each strategy. For all strategies, the model is meshed into $10 \times 1$ shell elements; and each shell element has $5 \times 3$ nodes. This meshing proves convergent for all strategies, as shown in section 3.3.1.

From classic beam theory, the deflection at free end of a uniform cantilever is $\delta = \frac{Pl^3}{3EI}$, where $L$ is length of cantilever, $P$ is the applied force at the free end, and $I$ is the cross-section moment inertial. Results obtained from beam theory and the three strategies are provided in Table 3.1.

Table 3.1: Deflections at the free end obtained from beam theory and strategies for example 1

| Loads (lb.) | Beam Theory ($in^{-3}$) | Function driven ($in^{-3}$) | Global node driven ($in^{-3}$) | Element driven ($in^{-3}$) |
|---|---|---|---|---|
| 0.05 | 125 | 125.602 | 125.602 | 125.602 |
| 0.10 | 250 | 251.204 | 251.204 | 251.204 |
| 0.15 | 375 | 376.806 | 376.806 | 376.806 |
| 0.20 | 500 | 502.408 | 502.407 | 502.408 |
| 0.25 | 625 | 628.009 | 628.009 | 628.009 |
| 0.30 | 750 | 753.611 | 753.611 | 753.611 |
| 0.35 | 875 | 879.213 | 879.213 | 879.213 |
| 0.40 | 1000 | 1004.815 | 1004.815 | 1004.815 |
| 0.45 | 1125 | 1130.417 | 1130.417 | 1130.417 |
| 0.50 | 1250 | 1256.019 | 1256.019 | 1256.019 |

As clearly shown in the table, results obtained from the three strategies are identical in this example that has no material grading. The results from three strategies are very close to those from beam theory as the difference with beam theory is only 0.482%.

Figure 3.7 shows the load-deflection curve obtained from the three strategies and from beam theory. As can be seen, the solutions are identical.

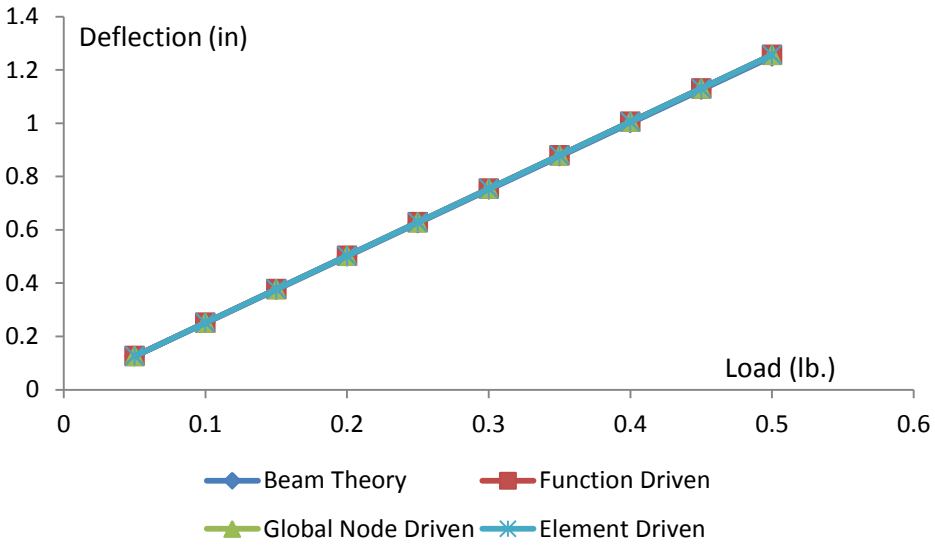


Figure 3.7: Deflections versus loads from beam theory and strategies for example 1

### 3.2.2 Verifications using uniform grading (Example 2)

Here we consider example 2 that is of a beam with uniform grading. For all strategies, the model is meshed into $10 \times 1$ shell elements; and each shell element has $5 \times 3$ nodes. This meshing proves convergent for all strategies as shown in section 3.3.2.

The solution to this problem based on beam theory is given in the Appendix. The calculated deflection of the cantilever at its free end is equal to $3.65582P$. Results obtained from beam theory and the three strategies are given in Table 3.2. Since results from global node driven

strategies and element driven strategy are identical, results of those two strategies are provided in the same column.

Table 3.2: Deflections at the free end obtained from beam theory and strategies for example 2

| Load ($lb.$) | Beam theory ($in^{-3}$) | Global node driven ($in^{-3}$) (Element driven) | Function driven ($in^{-3}$) |
|---|---|---|---|
| 0.02 | 73.116 | 73.585 | 73.538 |
| 0.04 | 146.233 | 147.176 | 147.102 |
| 0.06 | 219.349 | 220.579 | 220.558 |
| 0.08 | 292.465 | 294.177 | 294.283 |
| 0.10 | 365.582 | 367.628 | 367.927 |
| 0.12 | 438.698 | 441.243 | 441.228 |
| 0.14 | 511.814 | 514.624 | 514.774 |
| 0.16 | 584.930 | 588.219 | 588.361 |
| 0.18 | 658.047 | 661.892 | 661.848 |
| 0.20 | 731.163 | 735.235 | 735.372 |
| 0.22 | 804.279 | 809.398 | 809.297 |
| 0.24 | 877.396 | 882.664 | 882.715 |

Since material properties linearly vary along the length and the shape functions are fourth-order, material properties of integration points obtained from interpolation will be exact and identical to those obtained from visiting the grading functions. Hence, one can expect that the difference between the results from different strategies would be minimal, which is clearly indicated in Table 3.2. The results from all strategies are very close to those from beam theory. The difference of results between the global node driven (element driven) and beam theory is 0.643%, and the difference of results between the function driven strategy and beam theory is 0.577%.

Figure 3.8 shows the load-deflection relations obtained from the three strategies and beam theory. As can be seen, the solutions are almost identical.

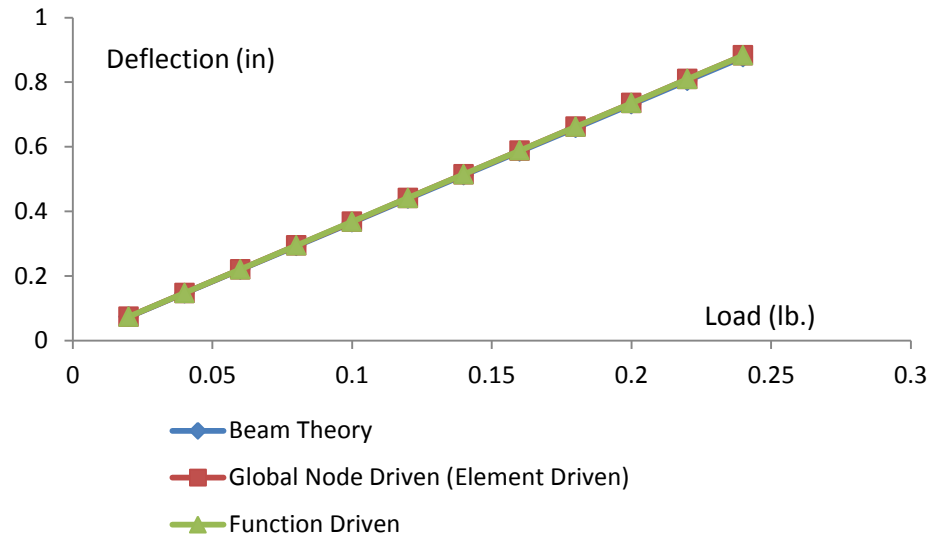


Figure 3.8: Deflections versus loads from beam theory and all strategies for example 2

### 3.2.3 Verifications using the two component beam (Example 3)

The problem considered here is of a cantilever made of two distinct parts as described by Example 3. For all strategies, the model is meshed into $10 \times 1$ shell elements, and each shell element has $5 \times 3$ nodes. This meshing proves convergent for all strategies, as shown in section 3.3.3.

The solution to this problem based on beam theory is given in the Appendix. The calculated deflection of the cantilever at its free end is equal to $4.752P$. Results obtained from beam theory and strategies are given in Table 3.3.

Table 3.3: Deflections at the free end obtained from beam theory and strategies for example 3

| Load (*lb.*) | Beam theory ($in^{-3}$) | Function driven ($in^{-3}$) | Global node driven ($in^{-3}$) | Element driven ($in^{-3}$) |
|---|---|---|---|---|
| 0.05 | 237.6 | 238.774 | 240.562 | 237.592 |
| 0.10 | 475.2 | 477.539 | 481.144 | 475.154 |
| 0.15 | 712.8 | 716.309 | 721.285 | 713.729 |

| | | | | |
|---|---|---|---|---|
| 0.20 | 950.4 | 995.079 | 961.956 | 991.805 |
| 0.25 | 1188.0 | 1193.848 | 1202.831 | 1189.995 |
| 0.30 | 1425.6 | 1432.618 | 1443.425 | 1428.352 |
| 0.35 | 1663.2 | 1671.388 | 1683.905 | 1666.339 |
| 0.40 | 1900.8 | 1910.157 | 1924.441 | 1904.612 |
| 0.45 | 2138.4 | 2148.927 | 2165.109 | 2143.029 |
| 0.50 | 2376.0 | 2387.696 | 2405.607 | 2381.353 |

The results from these strategies are very close to those from beam theory. However, one can observe that the global node driven strategy generates bigger difference with respect to beam theory than the other two strategies. The reason for this will be further discussed in section 3.4.2. The average differences of the global node driven, the element driven and the function driven strategies with respect to beam theory are, respectively, 1.23%, 0.56%, and 0.79%.

Figure 3.9 shows the load-deflection relations obtained from the three strategies and beam theory. As can be seen, the solutions are almost identical.

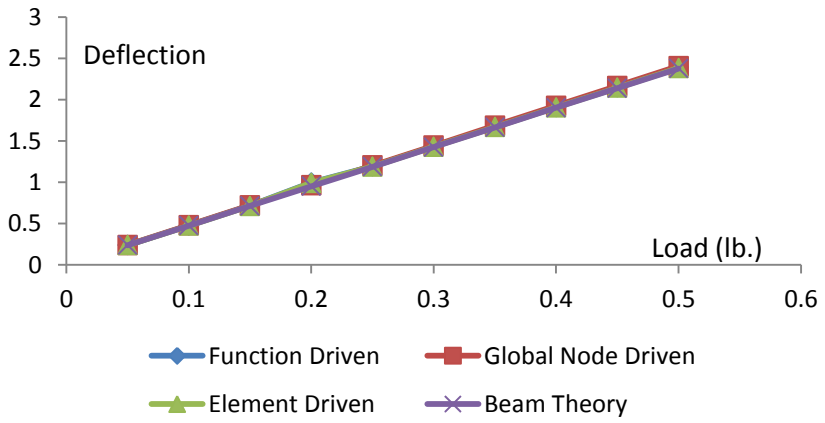


Figure 3.9: Deflections versus loads from beam theory and strategies for example 3

**Conclusion:**

Three examples are analyzed by beam theory and using the three strategies. As shown in each of the three examples, the results obtained from the three strategies are close to the results obtained from beam theory. This indicates that the implementations for the three strategies in FE program produce accurate linear results when compared to beam theory.

## 3.3 Convergence of finite element solutions

The following is a convergence study for the three examples described. In each case the base FEM is the solution for elements with uniform material properties. The exact solution is from beam theory.

### 3.3.1 Convergence of the uniform cantilever (Example 1)

Since in the uniform cantilever all material properties are constant over the cantilever, all strategies will result in exactly the same properties at the integration points during the FEA solution. Therefore, it is reasonable to presume that results of these four cases should converge at the same rate. As a result, for the same mesh nodes and elements, the results from these four cases are identical.

As shown in the Figure 3.10, for $3 \times 3$ nodes per element, results tend to converge after $M = 4$ elements in the length. Figure 3.8 and 3.9, for $4 \times 3$ and $5 \times 3$ nodes per element, show that results begin to converging at $M = 2$. Given $M = 10$, the convergence rates of $m = 3, 4, 5, 6$ nodes per element is also investigated and shown in Figure 3.13. Therefore, given ten elements along the length, the FE model will converge even for the lower order elements.

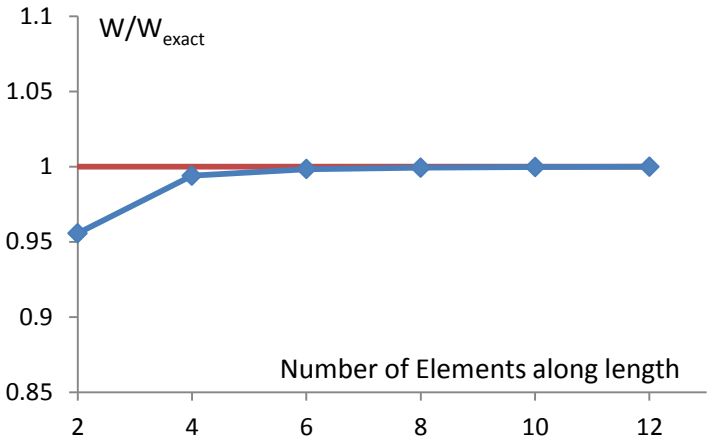


Figure 3.10: Convergence of 3 × 3 nodes per element

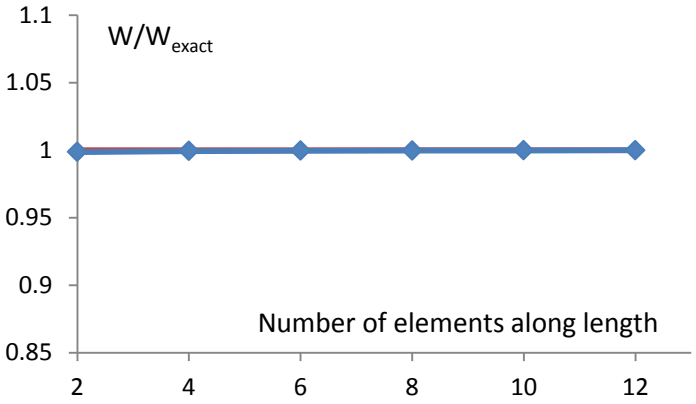


Figure 3.11: Convergence of 4 × 3 nodes per element

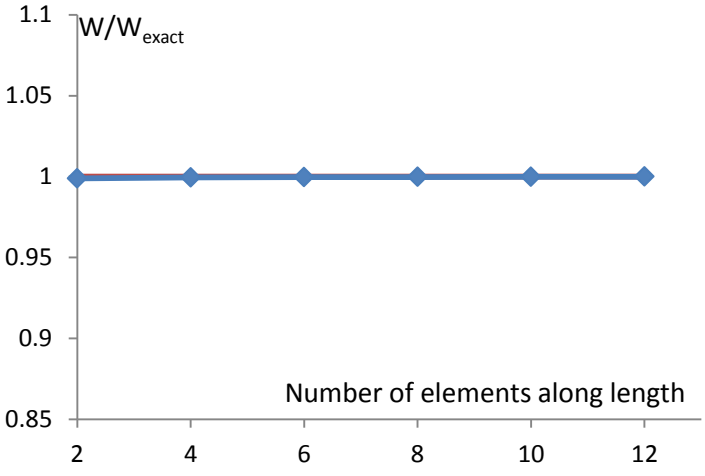


Figure 3.12: Convergence of 5 × 3 nodes per element

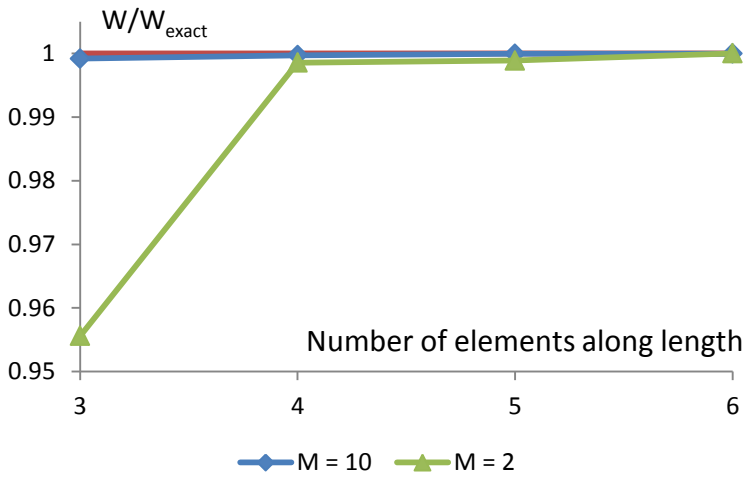


Figure 3.13: Convergence rate with $M = 2, 10$ and $m = 3, 4, 5, 6$

### 3.3.2 Convergence of uniform graded cantilever (Example 2)

For the uniformly graded cantilever of Example 2, given the same order and amount of elements, the results from all three strategies are almost identical. This is because the properties are calculated exactly by all three strategies. The results obtained from base FE analysis are different since the properties are not exact. The convergence rates of the three strategies and base FE analysis are shown in Figures 3.14, 3.15 and 3.16.

As shown in the Figure 3.14, for $3 \times 3$ nodes per element, results tend to converge after $M = 3$ for all strategies, while results from base FE analysis do not converge until $M = 5$.

In the Figure 3.15 and 3.16, for $4 \times 3$ and $5 \times 3$ nodes per element, results begin converging at $M = 1$ for all strategies, while results from base FE analysis do not converge until $M = 5$.

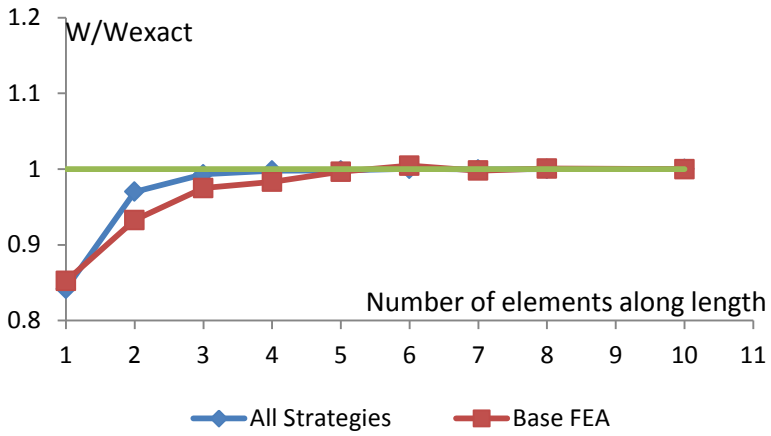


Figure 3.14: Convergence of 3 × 3 nodes per element

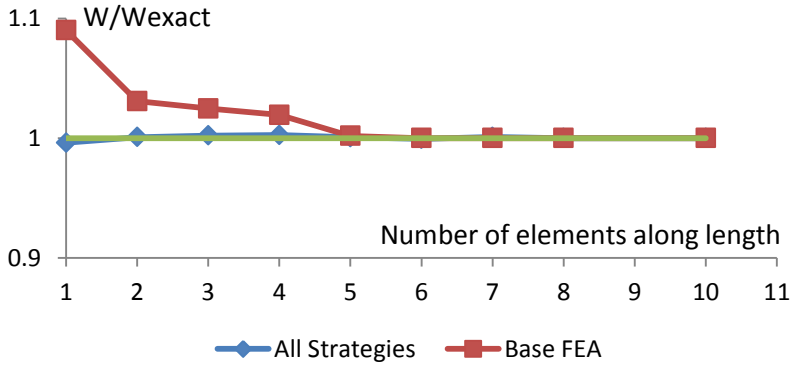


Figure 3.15: Convergence of 4 × 3 nodes per element

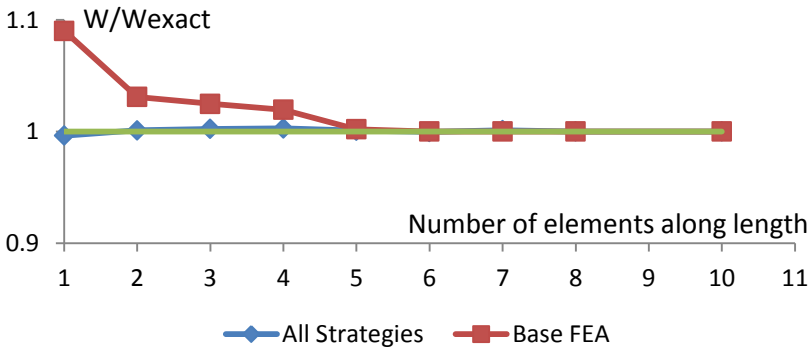


Figure 3.16: Convergence of 5 × 3 nodes per element

Figure 3.17 shows the convergence rates with $\mathrm{M} = 1, 2, 10$ and $\mathrm{m} = 3, 4, 5$. For one or two elements along the cantilever length, results converge at $\mathrm{m} = 4$ nodes along length of the element. Given ten elements along the cantilever length, results converge at $\mathrm{m} = 3$.

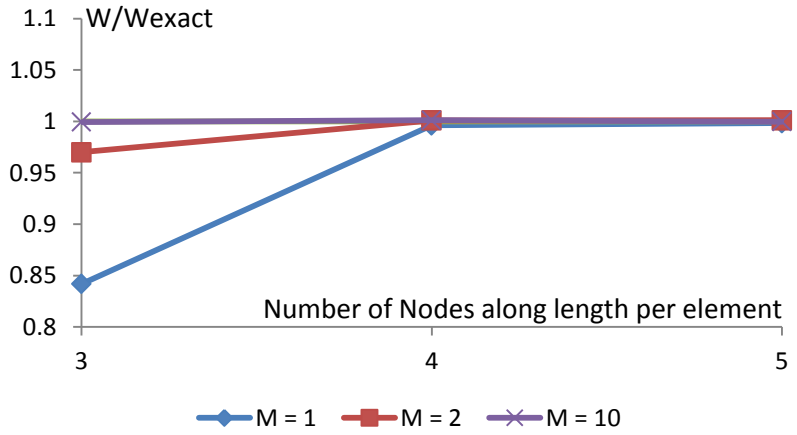


Figure 3.17: Convergence of strategies with $M = 1, 2, 10$ and $m = 3, 4, 5$

### 3.3.3 Convergence of two material cantilever (Example 3)

Here we consider Example 3 that has a cantilever made of two distinct materials. Figure 3.18, 3.19 and 3.20 show the convergence rates of $3 \times 3$, $4 \times 3$, $5 \times 3$ nodes per element, respectively.

As shown in Figure 3.18, the function driven strategy converges faster than the other two strategies and the base FEA. The global Node driven strategy slowly tends to converge. Base FEA and element driven strategies jump up and down before convergence. However, element driven strategy generates more accurate results than node driven strategy does. When there are even numbers of elements along length of cantilever, all strategies and the base FEA have more accurate values than when there are odd numbers of elements.

As shown in Figure 3.19, the function driven strategy tends to converge at less number of elements along length than the other strategies and base FEA do. Similar to Figure 3.18, when there are even numbers of elements along length of cantilever, all strategies and base FEA have more accurate values than when there are odd numbers of elements.

As shown in Figure 3.20, the element driven strategy and the function driven strategy have better convergence performance than the other two. Similar to Figure 3.18 and 3.19, all strategies and base FEA have more accurate values with even numbers of elements along length than odd numbers. However, the difference between even and odd numbers of elements becomes smaller than previous two cases.

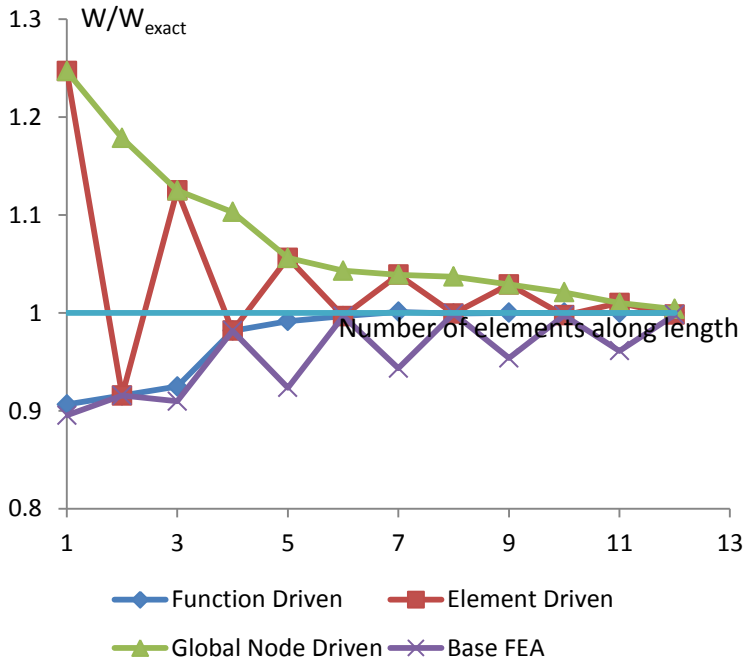


Figure 3.18: Convergence of 3 × 3 nodes per element

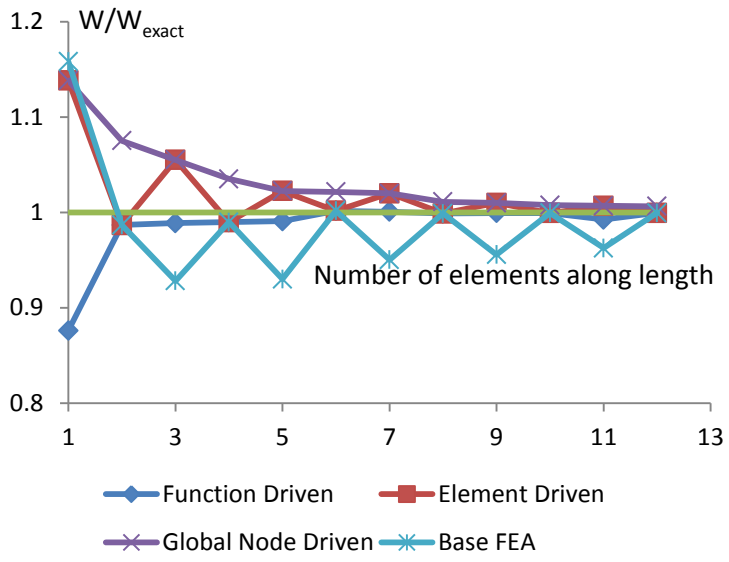


Figure 3.19: Convergence of $4 \times 3$ nodes per element

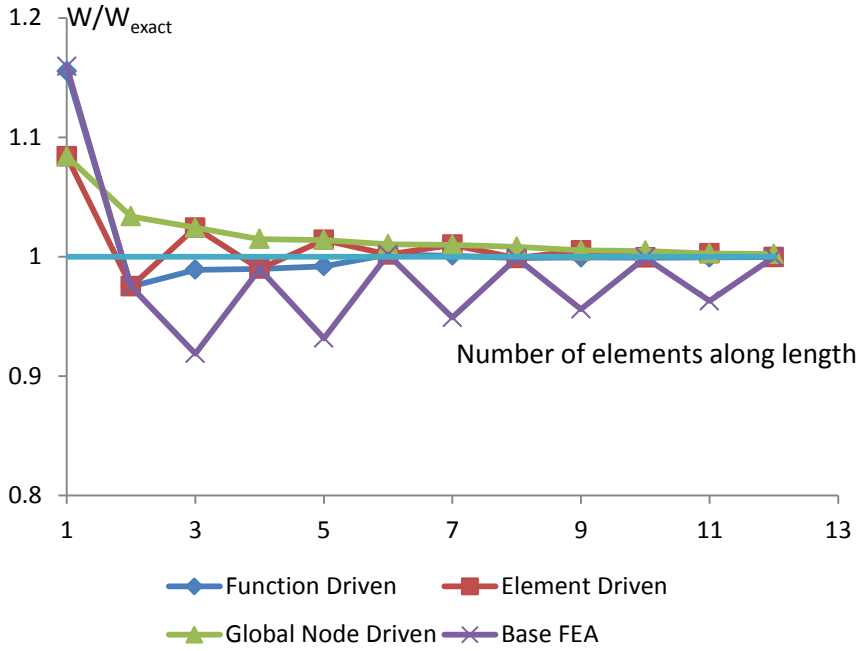


Figure 3.20: Convergence of $5 \times 3$ nodes per element

Figure 3.21 shows the convergence rates with $M = 5$ and $\mathrm{m} = 3, 4, 5$. The element driven and the global node driven strategies converge at the same rate with respect to increasing of

nodes. The function driven strategy and the base FEA is not sensitive to element orders at $M = 5$.

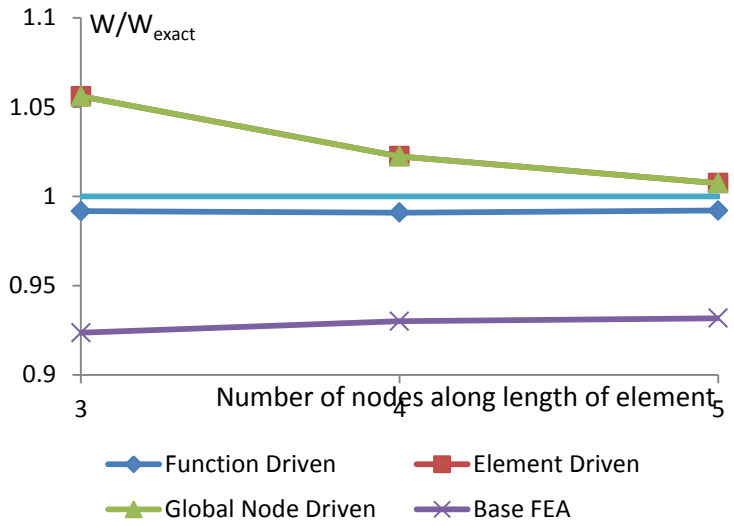


Figure 3.21: Convergence with $M = 5$ and $m = 3, 4, 5$

## 3.4 Comparisons of the strategies

### 3.4.1 Thickness grading in shells

For element driven and global node driven strategies, the elements obtain material properties through interpolation of the node properties. Strict implementation of these two strategies in shell elements does not allow material grading in the thickness since the nodes only exist at the mid-point of the shell thickness. This shortcoming can be solved through providing thickness variation as a part of nodal properties for the shell nodes.

The function driven strategy has no limitation to deal with problems with material grading in the thickness for shell element implementation.

For brick element implementation, all three strategies can be used to introduce material grading in thickness of the finite element model.

### 3.4.2 Comparisons between global node driven strategy and element driven strategy

If material properties gradually vary, the global node driven strategy and the element driven strategy can actually provide identical results. However, if there are material property jumps, the results obtained from the element driven strategy can accurately capture the jump if we put the element interface at the jump, but the global node driven strategy has no method to capture jumps. This section will describe this difference by comparing example 2 and 3 introduced in section 3.1.2 and 3.1.3.

**Gradual material grading:**

For gradual material grading, the global node driven strategy and element driven strategy have the same results in the FE analysis. Consider example 2 discussed in section 3.1.2. The global node and local node assignments, and elastic modulus diagram are shown in figure 3.22.

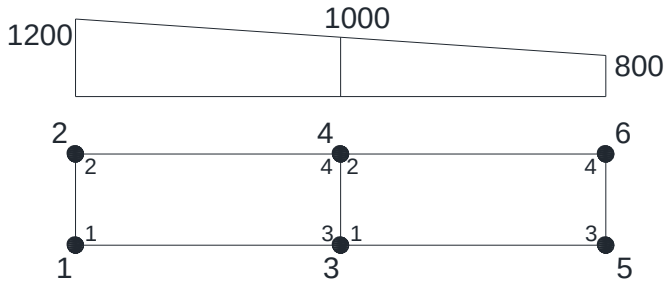


Figure 3.22: Local and global node assignments, elastic modulus diagram for example 2

Global nodes can be assigned with material properties as follows: 1(1200, 0.3), 2(1200, 0.3), 3(1000, 0.3), 4(1000, 0.3), 5(800, 0.3), 6(800, 0.3). Local nodes can have material

properties as follows: 1(1200, 0.3), 2(1200, 0.3), 3(1000, 0.3), 4(1000, 0.3) in element 1; 1(1000, 0.3), 2(1000, 0.3), 3(800, 0.3), 4(800, 0.3) in element 2.

Material properties obtained by interpolation of nodes are shown in Figures 3.23 and 3.24. Since the local nodes and the global nodes have the same properties, an integration point will obtain the same material properties from the two strategies as shown in Figures 3.23 and 3.24.

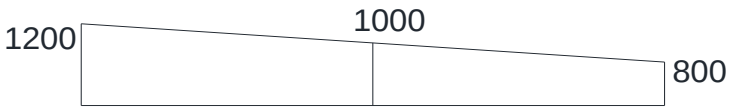


Figure 3.23: Interpolated material properties for global node driven strategy

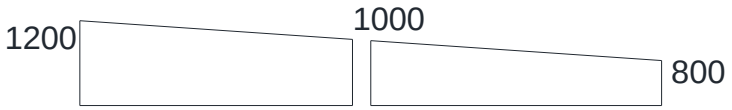


Figure 3.24: Interpolated material properties for element driven strategy

In the example 2, material properties are linear decrease along the length of cantilever, and the results obtained from the element driven and the global node driven strategies are identical.

**Material property jump:**

For material property jumps, the global node driven strategy has a difficulty capturing the exact properties. Consider example 3 discussed in section 3.1.3. The global node and local node assignments, and elastic modulus diagram are shown in Figure 3.25.

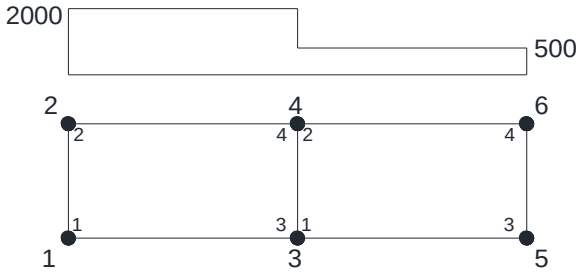


Figure 3.25: Local and global node assignments, elastic modulus diagram for example 3

The global nodes can be assigned with material properties as follows: 1(2000, 0.3), 2(2000, 0.3), 3(2000, 0.3), 4(2000, 0.3), 5(500, 0.3), 6(500, 0.3). Local nodes can have material properties as follows: 1(2000, 0.3), 2(2000, 0.3), 3(2000, 0.3), 4(2000, 0.3) in element 1; 1(500, 0.3), 2(500, 0.3), 3(500, 0.3), 4(500, 0.3) in element 2.

Material properties obtained by interpolation of nodes are shown in Figures 3.26 and 3.27. Since local nodes and global nodes have different material properties, integration points get different material properties from the two strategies as shown in Figure 3.26 and 3.27.

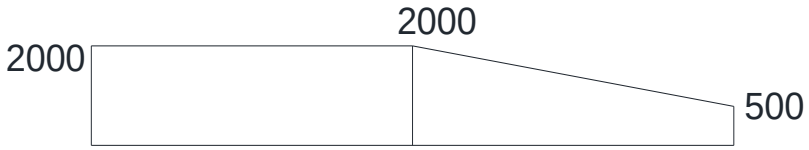


Figure 3.26: Interpolated material properties from global node driven strategy

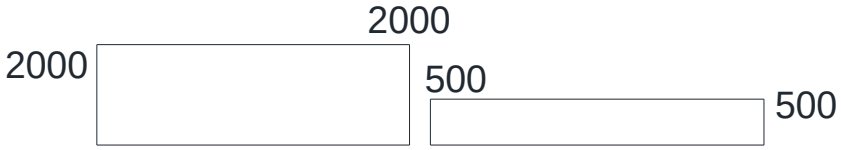


Figure 3.27: Interpolated material properties from element driven strategy

Local nodes can be assigned with material properties multiple times when belonging to different elements. Therefore, material property jumps can be accurately introduced into the finite element model by the way the element driven strategy assigns the properties. One can expect that as a result the element driven strategy will provides more accurate results.

In example 3, given that the FE model is meshed into $4 \times 1$ shell elements and each element has $4 \times 3$ nodes, the average differences of the global node drive strategy and element driven strategy with respect to beam theory are, respectively, 5.39% and 1.32%.

### 3.4.3 Memory usage

Let us consider the memory usage for the different strategies in the beam problem using shell elements. As shown in the Figure 3.28, the numbers of nodes along length and width directions of an element are $m$ and $n$, respectively. As shown in the Figure 3.29, the numbers of elements along the length and width directions are $M$ and $N$, respectively.

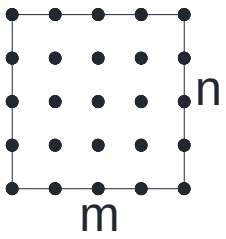


Figure 3.28: $m \times n$ nodes in an element (figure 3.1 repeated)

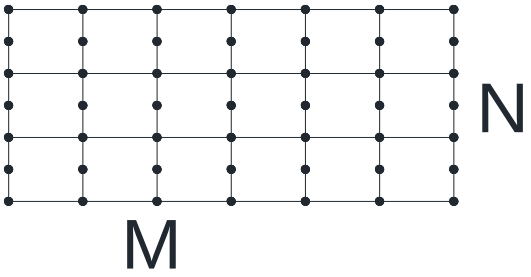


Figure 3.29: $M \times N$ elements in FE model (figure 3.2 repeated)

There are $\big((m-1) \times M + 1\big) \times \big((n-1) \times N + 1\big)$ global nodes; and the number of local nodes is $m \times n \times M \times N$. For the global node driven strategy each nodes needs to store properties of the node so each node will need additional memory equal to the space needed to store the properties. In the element driven strategy, each element needs to store properties for

each local node so that memory storage needs to be assigned in the size needed for the material properties at each local node. Therefore, the global node driven strategy requires the FE model to carry $\big((m-1)\times M+1\big)\times\big((n-1)\times N+1\big)$ pieces of material information, while the element driven strategy requires the FE model to carry $m\times n\times M\times N$ pieces of material information. If we subtract the memory needs of the two strategies we get that the element driven strategy needs $(MNm+MNn+M+N-Mm-Nn-MN-1)$ more pieces of material information than global node driven strategy does.

For the function driven strategy the FE model directly obtains the properties through defined functions so there is minimal storage need.

### 3.4.4 Comparisons between strategies and base FEA

In the case of constant material properties, the base FEA provides the same result as the three strategies do; therefore they converge at the same rate as shown in section 3.3.1.

In the case of gradual material grading, the global node driven strategy and element driven strategy provides identical results as discussed in section 3.4.2. The results from the three strategies are quite close as long as material grading matches the order of the interpolation of the elements. Otherwise, the function driven strategy provides more accurate properties. All three strategies converge faster than the base FEA.

In the case of material property jumps, generally speaking, the function driven strategy has the best convergence performance, the element driven strategy performs better than the global node driven strategy as discussed in section 3.4.2. The base FEA can only provide accurate results when the numbers of elements along length are even.

## 3.5 Conclusion

In this chapter three examples are analyzed. The first example is a cantilever with constant material properties. The second example is a cantilever with gradual material grading along the length direction. And the third example is a cantilever with material property jump along the length direction.

Each example is calculated through all three strategies. In the first example, results obtained from the three strategies are identical. In the second example, results obtained from element driven and global node driven strategies are identical. The results obtained from the three strategies are quite close. In the third example, the element driven strategy has more accurate results than the global node driven strategy does. In all three examples, the differences of three strategies with respect to beam theory are small once the number of elements or nodes in the elements increases to a point that the solutions converge.

In the convergence study, all strategies and the base FEA converge at the same rate in the case of constant material properties. With gradual material grading, the strategies have better convergence performance than base FEA. For the case of material jump, the base FEA can achieve results of high accuracy with even number of elements. Only function driven strategy shows obvious advantage to the base FEA with odd number of high order elements.

A set of comparisons is conducted. For shell element implementation, if there is material grading in thickness, the element driven and global node driven strategies are less applicable than the function driven strategy. In the case of gradual material grading, element driven and global node driven strategies have identical results. In the case of material property jump, the element driven strategy provides better results than the global node driven strategy. The element

driven strategy requires the FE model to carry more material information than the global node driven, while the function driven strategy does not require the FE model to carry material information.

# Chapter 4 Anisotropic elastic model and FEM implementation

This chapter develops a general finite deformation model for stress in order to deal with material grading in isotropic and anisotropic materials. Two examples are used to verify the implementation of this constitutive model.

As discussed in Chapter 1, an isotropic material has material grading only in the form of parameter scaling, while anisotropic materials also have grading associated with changing material orientation. Both geometrically linear and nonlinear behavior is considered in this chapter.

## 4.1 Constitutive model for anisotropic material grading

A constitutive model for anisotropic material grading, which is also applicable for isotropic materials, is developed herein.

### 4.1.1 Stress model

According to Negahban [24], a constitutive model for Cauchy stress $\boldsymbol{T}$ that captures finite isotropic and anisotropic elastic behavior can be written as

$$\boldsymbol{T}^{T} = \frac{1}{J}\boldsymbol{F}(\boldsymbol{C}:\boldsymbol{E})\boldsymbol{F}^{\boldsymbol{T}}, \tag{4.1}$$

where $\boldsymbol{C}$ is the fourth order tensor elastic moduli of the infinitesimal isotropic or anisotropic response, $\boldsymbol{F}$ is a second order tensor deformation gradient, $\boldsymbol{E}$ is a second order tensor Green strain

defined by $\boldsymbol{E} = \frac{1}{2}(\boldsymbol{F^T F} - \boldsymbol{I})$, in which $\boldsymbol{I}$ is the second order identity, $\boldsymbol{T}^T$ denotes transpose of Cauchy stress, $J$ is the volume ratio given by $J = det(\boldsymbol{F})$. The Cauchy stress can be obtained as

$$\boldsymbol{T} = \frac{1}{J}\boldsymbol{F}\,(\boldsymbol{C}\!:\!\boldsymbol{E})^T, \tag{4.2}$$

and the nominal stress $\boldsymbol{T}_0$ as

$$\boldsymbol{T}_0 = J\boldsymbol{F}^{-1}\boldsymbol{T} = (\boldsymbol{C}\!:\!\boldsymbol{E})^T\boldsymbol{F}^T. \tag{4.3}$$

Take time derivative of nominal stress to calculate the tangent modulus. This gives

$$\dot{\boldsymbol{T}}_0 = \overline{\dot{(\boldsymbol{C}\!:\!\boldsymbol{E})}^T}\boldsymbol{F}^T + (\boldsymbol{C}\!:\!\boldsymbol{E})^T\dot{\boldsymbol{F}}^T. \tag{4.4}$$

This can be written as

$$\dot{\boldsymbol{T}}_0 = (\mathbf{E1} + \mathbf{E2} + \mathbf{E3})\!:\!\dot{\boldsymbol{F}} \tag{4.5}$$

where $\mathbf{E1}$, $\mathbf{E2}$, and $\mathbf{E3}$ are fourth order tensors derived below. As a result, the target modulus is given by

$$\partial_{\boldsymbol{F}}(\boldsymbol{T}_0) = \mathbf{E1} + \mathbf{E2} + \mathbf{E3} \tag{4.6}$$

To calculate the three parts of the tangent modulus we complete the following steps. First we note

$$\boldsymbol{C}\!:\!\boldsymbol{E} = \left(C_{ijkl}\boldsymbol{e}_i \otimes \boldsymbol{e}_j \otimes \boldsymbol{e}_k \otimes \boldsymbol{e}_l\right)\!:\!(E_{mn}\boldsymbol{e}_m \otimes \boldsymbol{e}_n) = C_{ijkl}E_{kl}\boldsymbol{e}_i \otimes \boldsymbol{e}_j, \tag{4.7}$$

so

$$(\boldsymbol{C}\colon\boldsymbol{E})^T = C_{jikl}E_{kl}\boldsymbol{e}_i \otimes \boldsymbol{e}_j, \tag{4.8}$$

and

$$\overline{(\dot{\boldsymbol{C}}\colon\boldsymbol{E})^T}\boldsymbol{F}^T = \left(C_{jikl}\dot{E}_{kl}\boldsymbol{e}_i \otimes \boldsymbol{e}_j\right)(F_{nm}\boldsymbol{e}_m \otimes \boldsymbol{e}_n) = C_{jikl}F_{nj}\dot{E}_{kl}\boldsymbol{e}_i \otimes \boldsymbol{e}_n, \tag{4.9}$$

with

$$\dot{E}_{kl} = \frac{1}{2}\left(\dot{F}_{ok}F_{ol} + F_{ok}\dot{F}_{ol}\right). \tag{4.10}$$

This gives

$$\overline{(\dot{\boldsymbol{C}}\colon\boldsymbol{E})^T}\boldsymbol{F}^T = \tfrac{1}{2}C_{jikl}F_{nj}\dot{F}_{ok}F_{ol}\boldsymbol{e}_i \otimes \boldsymbol{e}_n + \tfrac{1}{2}C_{jikl}F_{nj}F_{ok}\dot{F}_{ol}\boldsymbol{e}_i \otimes \boldsymbol{e}_n. \tag{4.11}$$

We note that

$$\tfrac{1}{2}C_{jikl}F_{nj}\dot{F}_{ok}F_{ol}\boldsymbol{e}_i \otimes \boldsymbol{e}_n = \left(\tfrac{1}{2}C_{jikl}F_{nj}F_{ol}\boldsymbol{e}_i \otimes \boldsymbol{e}_n \otimes \boldsymbol{e}_o \otimes \boldsymbol{e}_k\right)\colon\left(\dot{F}_{ab}\boldsymbol{e}_a \otimes \boldsymbol{e}_b\right), \tag{4.12}$$

$$\tfrac{1}{2}C_{jikl}F_{nj}F_{ok}\dot{F}_{ol}\boldsymbol{e}_i \otimes \boldsymbol{e}_n = \left(\tfrac{1}{2}C_{jikl}F_{nj}F_{ok}\boldsymbol{e}_i \otimes \boldsymbol{e}_n \otimes \boldsymbol{e}_o \otimes \boldsymbol{e}_l\right)\colon\left(\dot{F}_{ab}\boldsymbol{e}_a \otimes \boldsymbol{e}_b\right), \tag{4.13}$$

so that

$$\overline{(\dot{\boldsymbol{C}}\colon\boldsymbol{E})^T}\boldsymbol{F}^T = (\mathbf{E1} + \mathbf{E2})\colon\dot{\boldsymbol{F}}. \tag{4.14}$$

If we define two fourth order tensors **E1** and **E2**

$$\mathbf{E1} = \frac{1}{2}C_{jikl}F_{nj}F_{ol}\boldsymbol{e}_i \otimes \boldsymbol{e}_n \otimes \boldsymbol{e}_o \otimes \boldsymbol{e}_k, \tag{4.15}$$

and

$$\mathbf{E2} = \frac{1}{2}C_{jikl}F_{nj}F_{ok}\boldsymbol{e}_i \otimes \boldsymbol{e}_n \otimes \boldsymbol{e}_o \otimes \boldsymbol{e}_l. \tag{4.16}$$

We also note that

$$(\boldsymbol{C}:\boldsymbol{E})^T\dot{\boldsymbol{F}}^T = C_{jikl}E_{kl}\dot{F}_{nj}\boldsymbol{e}_i \otimes \boldsymbol{e}_n, \tag{4.17}$$

which can be written as

$$C_{jikl}E_{kl}\dot{F_{nJ}}\boldsymbol{e}_i \otimes \boldsymbol{e}_n = \left(C_{jikl}E_{kl}\delta_{mn}\boldsymbol{e}_i \otimes \boldsymbol{e}_n \otimes \boldsymbol{e}_m \otimes \boldsymbol{e}_j\right):\left(\dot{F_{ab}}\boldsymbol{e}_a \otimes \boldsymbol{e}_b\right). \tag{4.18}$$

which can be written as

$$(\boldsymbol{C}:\boldsymbol{E})^T\dot{\boldsymbol{F}}^T = \mathbf{E3}:\dot{\boldsymbol{F}} \tag{4.19}$$

for

$$\mathbf{E3} = C_{jikl}E_{kl}\delta_{mn}\boldsymbol{e}_i \otimes \boldsymbol{e}_n \otimes \boldsymbol{e}_m \otimes \boldsymbol{e}_j. \tag{4.20}$$

### 4.1.2 Matrix form of elasticity tensor

Elasticity tensor $\boldsymbol{C}$ is a fourth order tensor, and can be expressed as $\boldsymbol{C} = C_{ijkl}e_i \otimes e_j \otimes e_k \otimes e_l$. The components of elasticity tensor have the properties $C_{ijkl} = C_{jikl} = C_{ijlk} = C_{klij}$, and hence the number of independent components is reduced from 81 to 21.

The components of elasticity tensor are often written in the form of the matrix

$$\left[C_{ijkl}\right] = \begin{bmatrix} C_{1111} & C_{1122} & C_{1133} & C_{1123} & C_{1131} & C_{1112} \\ C_{2211} & C_{2222} & C_{2233} & C_{2223} & C_{2231} & C_{2212} \\ C_{3311} & C_{3322} & C_{3333} & C_{3323} & C_{3331} & C_{3312} \\ C_{2311} & C_{2322} & C_{2333} & C_{2323} & C_{2331} & C_{2312} \\ C_{3111} & C_{3122} & C_{3133} & C_{3123} & C_{3131} & C_{3112} \\ C_{1211} & C_{1222} & C_{1233} & C_{1223} & C_{1231} & C_{1212} \end{bmatrix}. \tag{4.21}$$

Many papers use an index mapping standard to reconstruct the component matrix of elasticity tensor, that is

$$\begin{array}{cccccccc} ij & = & 11 & 22 & 33 & 23,32 & 13,31 & 12,21 \\ \Downarrow & & \Downarrow & \Downarrow & \Downarrow & \Downarrow & \Downarrow & \Downarrow \\ \alpha & = & 1 & 2 & 3 & 4 & 5 & 6 \end{array}. \tag{4.22}$$

As a result of this transformation, the elasticity tensor is frequently written as

$$\begin{bmatrix} C_{11} & C_{12} & C_{13} & C_{14} & C_{15} & C_{16} \\ C_{12} & C_{22} & C_{23} & C_{24} & C_{25} & C_{26} \\ C_{13} & C_{23} & C_{33} & C_{34} & C_{35} & C_{36} \\ C_{14} & C_{24} & C_{34} & C_{44} & C_{45} & C_{46} \\ C_{15} & C_{25} & C_{35} & C_{45} & C_{55} & C_{56} \\ C_{16} & C_{26} & C_{36} & C_{46} & C_{56} & C_{66} \end{bmatrix}. \tag{4.23}$$

### 4.1.3 Elasticity matrix for different materials symmetries

The matrixes of elasticity constants for several of the most typical materials are briefly introduced here.

**Isotropic material**

An isotropic material has full symmetry along all directions. There are only two independent material coefficients for an isotropic infinitesimal elastic materials and the elasticity matrix is given by

$$\begin{bmatrix} 2G+\lambda & \lambda & \lambda & & & \\ \lambda & 2G+\lambda & \lambda & & 0 & \\ \lambda & \lambda & 2G+\lambda & & & \\ & & & G & 0 & 0 \\ & 0 & & 0 & G & 0 \\ & & & 0 & 0 & G \end{bmatrix}, \tag{4.24}$$

in which, $\lambda$ and $G$ are the two Lamé constant ($G$ is shear modulus).

**Orthotropic material**

Materials that have three mutually orthogonal directions of preferred symmetry are called orthotropic materials. The components of the elasticity matrix in this case reduce to 9 independent terms and are given as

$$\begin{bmatrix} \mu_{11} & \mu_{12} & \mu_{13} & & & \\ \mu_{12} & \mu_{22} & \mu_{23} & & 0 & \\ \mu_{13} & \mu_{23} & \mu_{33} & & & \\ & & & \mu_{44} & 0 & 0 \\ & 0 & & 0 & \mu_{55} & 0 \\ & & & 0 & 0 & \mu_{66} \end{bmatrix}. \tag{4.25}$$

in which $\mu_{ij}$ are material parameters describing the orthotropic properties.

**Transversely isotropic material**

As a special class of orthotropic materials, transversely isotropic materials have the same properties in one plane, but different properties in the normal direction to that plane. Material properties of transversely isotropic materials can be described by 5 independent parameters. For transverse isotropy around the axis $\boldsymbol{e_3}$, the elasticity matrix is given as

$$\begin{bmatrix} \mu_{11} & \mu_{12} & \mu_{13} & & & \\ \mu_{12} & \mu_{11} & \mu_{13} & & 0 & \\ \mu_{13} & \mu_{13} & \mu_{33} & & & \\ & & & \mu_{44} & 0 & 0 \\ & 0 & & 0 & \mu_{44} & 0 \\ & & & 0 & 0 & \frac{1}{2}(\mu_{11} - \mu_{12}) \end{bmatrix}. \tag{4.26}$$

in which, $\mu_{ij}$ are material parameters representing the infinitesimal elastic response.

### 4.1.4 Matrix form of elasticity tensor for material grading

As discussed, graded materials may have material grading in the forms of parameter scaling or orientation changing. Those two types of material grading can be introduced by variations of elasticity tensors.

**Isotropic materials**

The isotropic material is a special case of the anisotropic material that has an elasticity matrix that is the same for all orientations. For example, in the linear grade example of the last chapter (Example 2), the grading was given by the elastic modulus $E(x) = 800\ (1 + 0.05\ x_1)$. The component matrix of elastic constants in this case will be

$$\begin{bmatrix} 1076.9\ (1+0.05\ x_1) & 461.5(1+0.05\ x_1) & 461.5(1+0.05\ x_1) & & & \\ 461.5(1+0.05\ x_1) & 1076.9\ (1+0.05\ x_1) & 461.5(1+0.05\ x_1) & & 0 & \\ 461.5(1+0.05\ x_1) & 461.5(1+0.05\ x_1) & 1076.9\ (1+0.05\ x_1) & & & \\ & & & 307.7(1+0.05\ x_1) & 0 & 0 \\ & 0 & & 0 & 307.7(1+0.05\ x_1) & 0 \\ & & & 0 & 0 & 307.7(1+0.05\ x_1) \end{bmatrix}. \quad (4.27)$$

**Anisotropic materials**

**Material grading of parameters**

For anisotropic materials, the material grading might keep the orientation of the anisotropy the same, but vary the parameters. In this case the properties are scaled only. Since there are more parameters describing an anisotropic material, the number of parameters that can be graded will be larger.

**Material grading of orientations**

As discussed above, anisotropic materials may have material grading in the form of changing orientation of the anisotropy. Material orientation grading can also be expressed by variations of elasticity tensor, but these changes have to be consistent with the changing orientation of the anisotropy. It is simpler to directly rotate the properties as described below.

As an example, consider a composite plate that is made of orthotropic laminas. One layer of lamina is shown in Figure 4.1. Let $(x - y - z)$ denote the global coordinate system for the composite plate, and let $(x_1 - x_2 - x_3)$ denote the coordinates along the principal directions of anisotropy. As can be seen in Figure 4.1, in this example $x_3$ and $z$ coincide and the angles of $(x, x_1)$ and $(y, x_2)$ are θ.

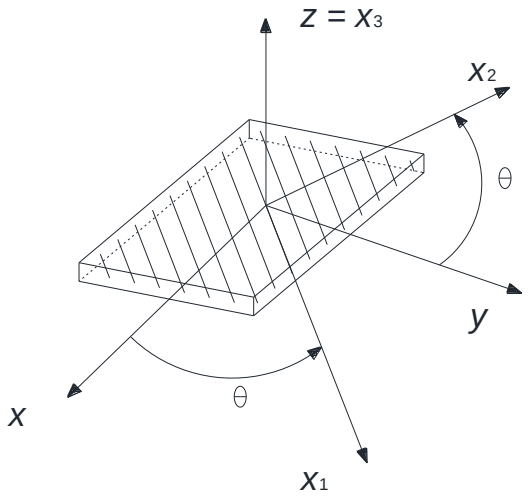


Figure 4.1: A lamina with material principal and global coordinate systems

Let $C$ denote the matrix form of the components elasticity tensor $\boldsymbol{C}$ with respect to material principal coordinates. Let $C'$ denote the matrix form of elasticity tensor with respect to global coordinates. These are related by the relation

$$C' = TCT^T, \tag{4.28}$$

in which, $T$ is transformation matrix. For the rotation angle $\theta$ described above, the transformation matrix is

$$\begin{bmatrix} cos^2\theta & sin^2\theta & 0 & 0 & 0 & -sin2\theta \\ sin^2\theta & cos^2\theta & 0 & 0 & 0 & sin2\theta \\ 0 & 0 & 1 & 0 & 0 & 0 \\ 0 & 0 & 0 & cos\theta & sin\theta & 0 \\ sin^2\theta & cos^2\theta & 0 & -sin\theta & cos\theta & 0 \\ sin\theta cos\theta & -sin\theta cos\theta & 0 & 0 & 0 & cos^2\theta - sin^2\theta \end{bmatrix}. \quad (4.29)$$

In the graded material the angle $\theta$ expresses the orientation grading, which can be defined as function of positions so that $\theta(\boldsymbol{X})$. Therefore, the transformation matrix in this case becomes a functions of positions so that $T_{ij}(\boldsymbol{X})$. This is the method to describe material orientation grading into the elasticity tensor.

The transformation matrix given above is for rotation around the $x_3$ axis. Transformation matrixes along the other two axes are available in literatures.

### 4.1.5 Discussion

The proposed constitutive model is a finite deformation anisotropic elastic response model, but which builds on parameters redly available for infinitesimal elastic response. In the work in finite element methods for infinitesimal deformations, it is popular to define the stress is in the form $\boldsymbol{\sigma} = \boldsymbol{C\varepsilon}$, in which $\boldsymbol{\sigma}$ is six-dimensional stress vector, $\boldsymbol{C}$ is elastic stiffness matrix and $\boldsymbol{\varepsilon}$ is the six-dimensional engineering strain vector. As a result, the values of $\boldsymbol{C}$ for many different materials are tabulated and can be directly used in this implementation to characterize the finite deformation response.

## 4.2 Verification of constitutive model

This section uses two examples to verify the constitutive model and finite element implementations.

### 4.2.1 Example 1: Isotropic plate with uniform distributed load

Here we consider an isotropic square plate under a uniformly distributed load and simple supports. The problem was conducted to verify the implementation. The plate has dimensions and material parameters $a = b = 10\ inch., h = 1\ inch, E = 7.8 \times 10^6\ psi, \nu = 0.3$. Two types of simply supported boundary conditions are used. Use $u_0$, $v_0$ and $w_0$ to denote the boundary displacements along $x$, $y$, and $z$ directions, respectively. As shown in Figure 4.2, the displacement boundary conditions for SS-1 and SS-2 are separately

$$\text{SS-1:}\quad \text{at } x = \pm\frac{a}{2}\text{: } v_0 = w_0 = 0$$

$$\text{at } y = \pm\frac{a}{2}\text{: } u_0 = w_0 = 0,$$

$$\text{SS-2:}\quad \text{at } x = \pm\frac{a}{2}\text{: } u_0 = v_0 = w_0 = 0$$

$$\text{at } y = \pm\frac{a}{2}\text{: } u_0 = v_0 = w_0 = 0$$

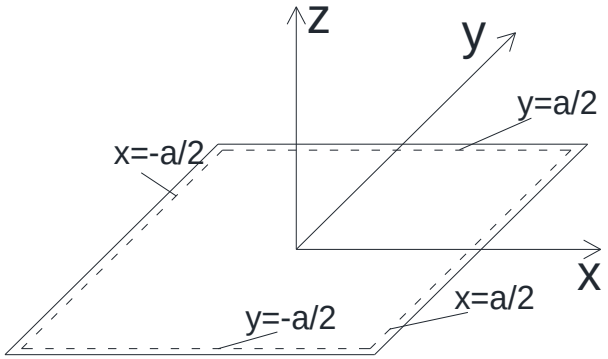


Figure 4.2: Boundary conditions of plate

The convergence rates for different order elements are shown in Figure 4.3. The FE model is meshed into $6 \times 6$ elements, and each element has either $3 \times 3$, $4 \times 4$, or $5 \times 5$ nodes.

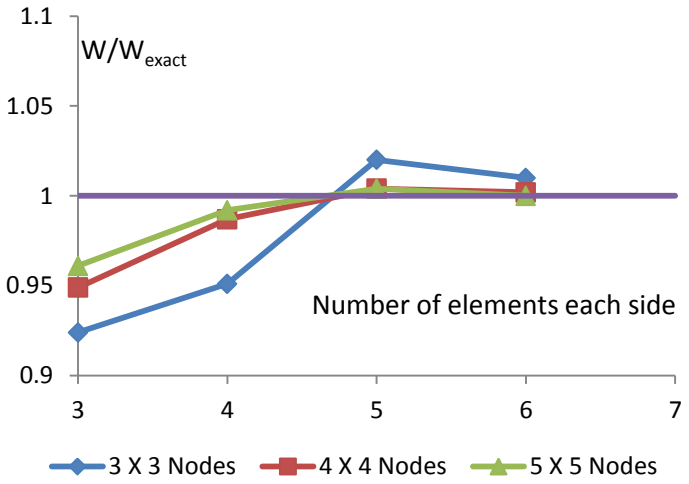


Figure 4.3: Convergence of FE model with different order elements for example 1

The entire plate is loaded with uniformly-distributed force $q_0$. Define a load parameter as $\overline{p} = q_0 a^4/Eh^4$. The center deflections under uniformly distributed loading are provided in Table 4.1.

Table 4.1: Center deflections of simply supported plates under load

| $\overline{p}$ | SS-1 (*in*) | SS-2 (*in*) |
|---|---|---|
| 6.25 | 0.2937 | 0.2723 |
| 12.50 | 0.5376 | 0.4543 |
| 25.00 | 0.8888 | 0.6812 |
| 50 | 1.3267 | 0.9470 |
| 75 | 1.6284 | 1.1227 |
| 100 | 1.8616 | 1.2582 |
| 125 | 2.0566 | 1.3705 |
| 150 | 2.2262 | 1.4675 |
| 175 | 2.3776 | 1.4675 |
| 200 | 2.5153 | 1.5537 |

As clearly shown in Figure 4.4, the nonlinear behaviors of the two simply-supported plates nearly coincide with the results by Reddy [20].

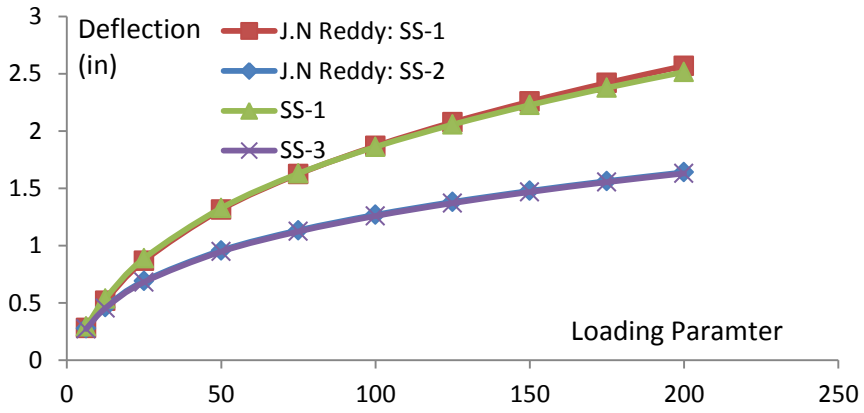


Figure 4.4: Center deflections versus loading parameter

### 4.2.2 Example 2: Anisotropic plate with uniform distribute load

Here we consider a simply supported orthotropic square plate under a uniform distributed load. The plate has dimensions and material parameters $a = b = 12\ inch, h = 0.138\ inch, E_1 = 3 \times 10^6\ psi, E_2 = 1.28 \times 10^6\ psi, E_3 = 1.28 \times 10^6\ psi, G_{12} = G_{13} = G_{23} = 0.37 \times 10^6\ psi, \nu_{12} = \nu_{13} = 0.32, \nu_{12} = 0.2.$

The distributed load is $q_0$ and directed perpendicular to the plate. Both simply supported boundary conditions shown in example 1 are used in this example.

The convergence rates for different order elements are shown in Figure 4.4. The FE model is meshed into $6 \times 6$ elements, and each element has either $3 \times 3$, $4 \times 4$, or $5 \times 5$ nodes. The center deflections under uniformly distributed loading are provided in Table 4.2.

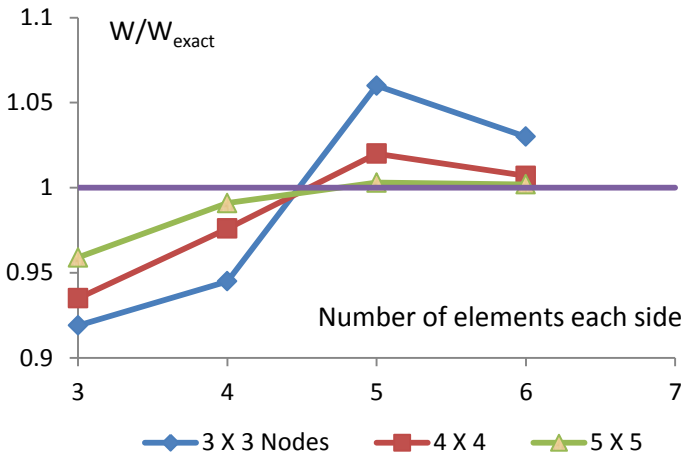


Figure 4.5: Convergence of FE model with different order elements

Table 4.2: Center deflections for simply supported orthotropic plates under uniform load

| $q_0$ (*psi*) | SS-1 (*in*) | SS-2 (*in*) |
|---|---|---|
| 0.05 | 0.0112 | 0.0111 |
| 0.10 | 0.0222 | 0.0215 |
| 0.20 | 0.0435 | 0.0392 |
| 0.40 | 0.0808 | 0.0642 |
| 0.60 | 0.1112 | 0.0815 |
| 0.80 | 0.1365 | 0.0949 |
| 1.00 | 0.158 | 0.1058 |
| 1.20 | 0.1767 | 0.1151 |
| 1.40 | 0.1934 | 0.1233 |
| 1.60 | 0.2085 | 0.1306 |
| 1.80 | 0.2223 | 0.1372 |
| 2.00 | 0.235 | 0.1432 |

As clearly shown in Figure 4.6, the nonlinear behaviors for the two simply-supported conditions closely match the results by Reddy [20].

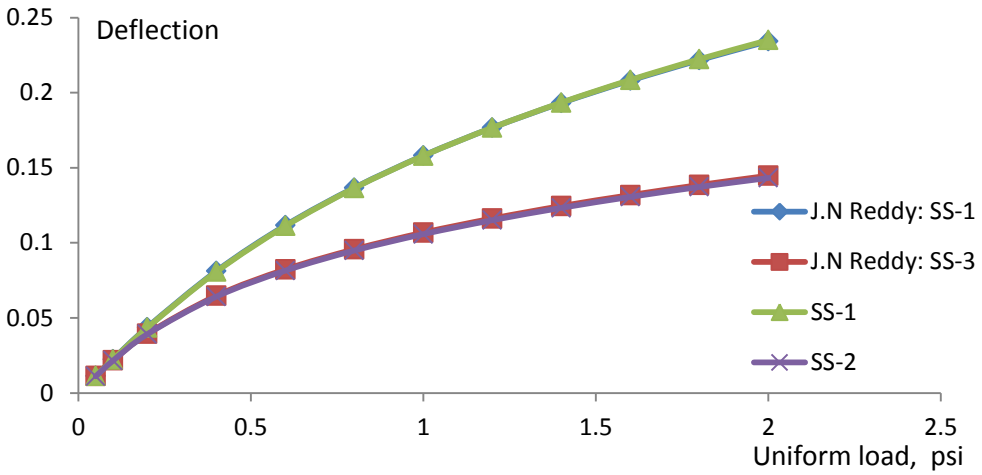


Figure 4.6: Center deflections versus uniformly distributed loads for example 2

Since the nonlinear behaviors of the two examples are very close to the results by J. N. Reddy [20], we consider the constitutive model and the implementation being correct for both isotropic and anisotropic materials in geometrically nonlinear analysis.

## 4.3 Conclusion

A constitutive model, which is applicable for both graded isotropic and anisotropic material grading, is proposed in this chapter. The full steps of constitutive model are calculated in details. Two examples are used to verify this constitutive model. These examples are isotropic plate and orthotropic plate, separately. Since the nonlinear behaviors obtained from constitutive model are very close to those by J. N. Reddy [20], the constitutive model proposed in this chapter is verified.

# Chapter 5 Examples of graded isotropic and anisotropic nonlinear elastic materials

In this chapter I will give examples of graded isotropic and anisotropic materials using the proposed anisotropic nonlinear elastic model.

## 5.1 Isotropic material with gradual grading in the thickness

In this example, the cantilever has dimensions of 1 in for the width, 1 in for the thickness and 10 in for the length. The bottom surface of the cantilever has elastic modulus $\mathrm{E_b} = 1000$ psi, and Poisson's ratio $\nu = 0.3$, while the tope surface has elastic modulus $\mathrm{E_t} = 2000$ psi, and Poisson's ratio $\nu = 0.3$. The elastic modulus of this cantilever linearly varies from the top surface to the bottom surface, as shown in Figure 5.1. Using $x$ to denote the vertical distance from the center line of the cross section, one can express the elastic modulus by the function $E(x) = E_t\left(\frac{x}{h} + \frac{1}{2}\right) - E_b(\frac{x}{h} - \frac{1}{2})$.

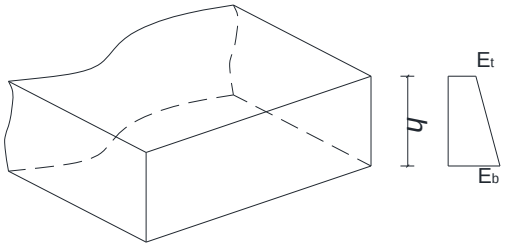


Figure 5.1: Elasticity modulus grading along thickness

As shown in Figure 5.2, a horizontal distributed force is applied at the free end of cantilever.

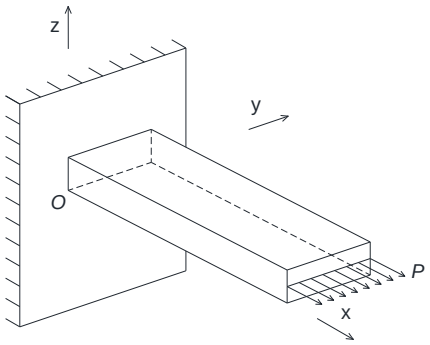


Figure 5.2: Horizontal loading at the free end of cantilever

For cantilever with uniform material properties, there should be no transverse deflection under axial force. However, due to the material grading in the thickness, the bottom part of the cross-section has higher elastic modulus, which makes it harder to extend under an axial force. The top part of the cross-section has lower elastic modulus, which makes it easier to extend under axial force. As a result, axial load on the beam results in transverse deflections of the end.

**Convergence study**

The convergence rates for different order shell and brick elements are shown in Figures 5.3 and 5.4. For the shell element, the model is meshed from$1 \times 1$ to $1 \times 10$ elements, and each element has $3 \times 3$ , $4 \times 4$ , or $5 \times 5$ nodes. For the brick element, the model is meshed into $5 \times 1 \times 2$ elements, and each element has $5 \times 3 \times 3$ nodes.

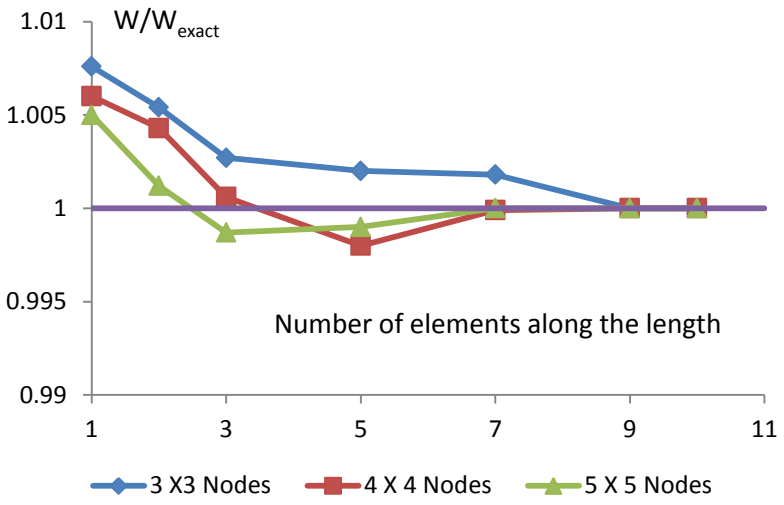


Figure 5.3: Convergence of different order of shell elements

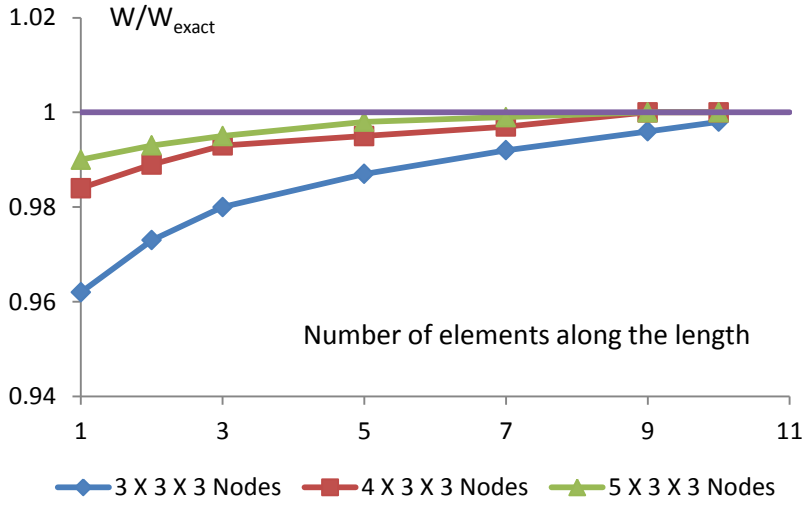


Figure 5.4: Convergence of different order of brick elements

**Linear Behavior**

In shell element model, function driven strategy is used. In brick element model, all three strategies are used. Since the results obtained from strategies are identical, results of those three strategies are provided in the same column. The results obtained from FE analysis are provided in Table 5.1. The relations between deflections versus loads are plotted in Figure 5.5.

Table 5.1: Deflections at free end of cantilever obtained from FE analysis

| Load (lb) | Brick | Shell |
|---|---|---|
| | All strategies ($in^{-3}$) | Function driven strategy ($in^{-3}$) |
| 2 | 46.150 | 46.124 |
| 4 | 92.301 | 92.305 |
| 6 | 138.451 | 138.457 |
| 8 | 184.602 | 184.609 |
| 10 | 230.752 | 230.761 |
| 12 | 276.902 | 276.913 |
| 14 | 323.053 | 323.066 |
| 16 | 369.203 | 369.218 |
| 18 | 415.354 | 415.304 |
| 20 | 461.504 | 461.523 |

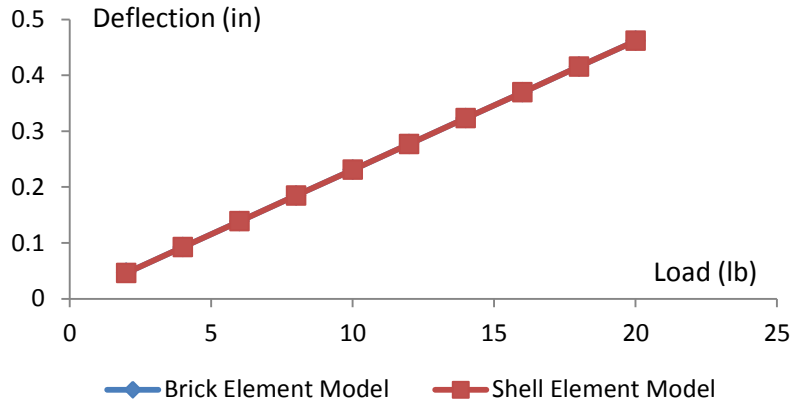


Figure 5.5: Deflections versus loads from brick and shell element models

The results from beam theory is also available in the Appendix, the deflection of cantilever at the free end is $\delta = 0.023077P$.

**Nonlinear behavior**

The nonlinear results of brick and shell element models for this example are provided in Table 5.2. The nonlinear behaviors of this example are shown in Figure 5.6. The linear and nonlinear behaviors of this example are shown in Figure 5.7.

Table 5.2: Free-end deflections considering geometric nonlinearity

| | Deflection ($in^{-3}$) | |
|---|---|---|
| Load (lb.) | Shell | Brick |
| 1 | 17.121 | 17.104 |
| 2 | 27.134 | 27.129 |
| 3 | 33.628 | 33.594 |
| 4 | 38.133 | 38.094 |
| 5 | 41.408 | 41.344 |
| 6 | 43.873 | 43.817 |
| 7 | 45.779 | 45.733 |
| 8 | 47.285 | 47.238 |
| 10 | 49.485 | 49.436 |
| 12 | 50.982 | 50.880 |
| 14 | 52.044 | 51.887 |
| 16 | 52.821 | 52.874 |
| 18 | 53.404 | 53.351 |
| 20 | 53.851 | 53.797 |

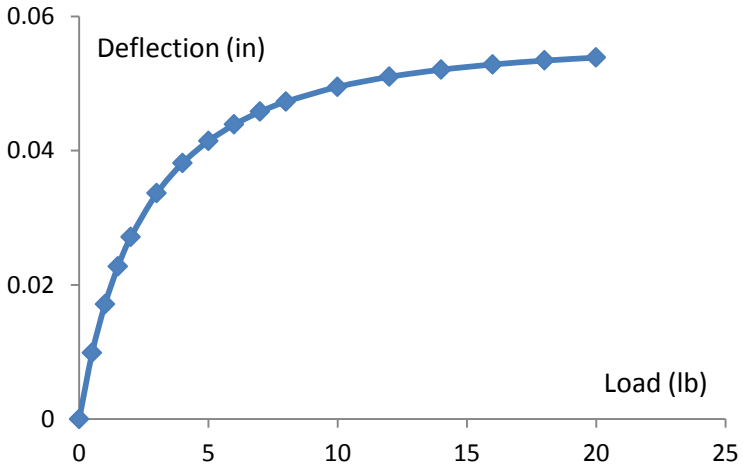


Figure 5.6: Nonlinear behaviors

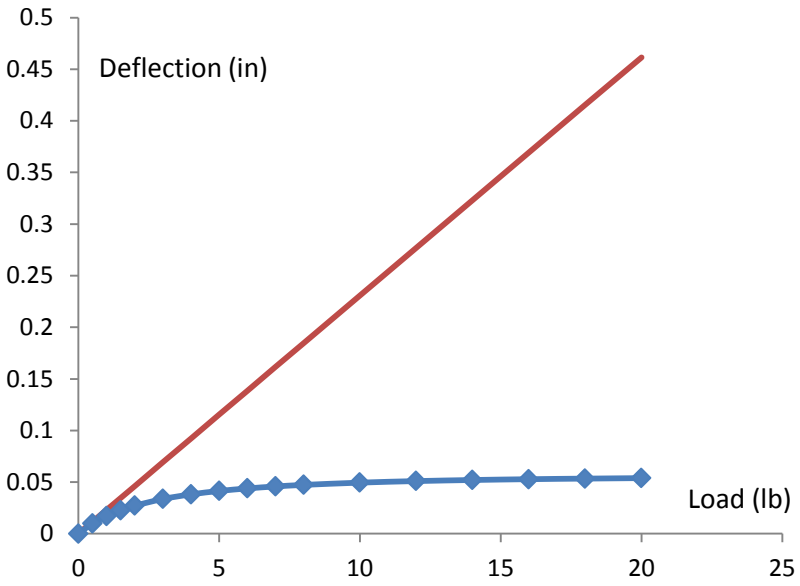


Figure 5.7: Linear and nonlinear behaviors

As shown in Figure 5.7, the deflection of the cantilever tends to stop increasing. This is because second order effect created by the deflection restricts further deflection.

## 5.2 Material orientation grading for anisotropic materials

Laminated composites are made of layers of orthotropic laminas, and a laminated composite plate usually has material orientation grading within the continuum.

We consider a cross-ply (0/90) laminated plate that is made of material with properties $E_1 = 40 \times 10^6\ psi, E_2 = 10^6\ psi, E_3 = 10^6\ psi, G_{12} = G_{13} = 0.6 \times 10^6\ psi, G_{23} = 0.5 \times 10^6\ psi, \nu_{12} = \nu_{13} = 0.25, \nu_{12} = 0.2$. The dimensions for plate are $a = b = 12\ inch$ for width and length, and $h = 0.3\ inch$ for thickness. The plate is clamped on the edges. This is given by the boundary conditions: at $x = \frac{a}{2}$: $u_0 = v_0 = w_0 = \emptyset_x = 0$, at $y = \frac{a}{2}$: $u_0 = v_0 = w_0 = \emptyset_y = 0$. A uniformly distributed load $q_0$ applies on the plate.

The convergence rate for shell model is shown in Figure 5.8. The model is meshed up to $6 \times 6$ shell elements, each element having up to $5 \times 5$ nodes.

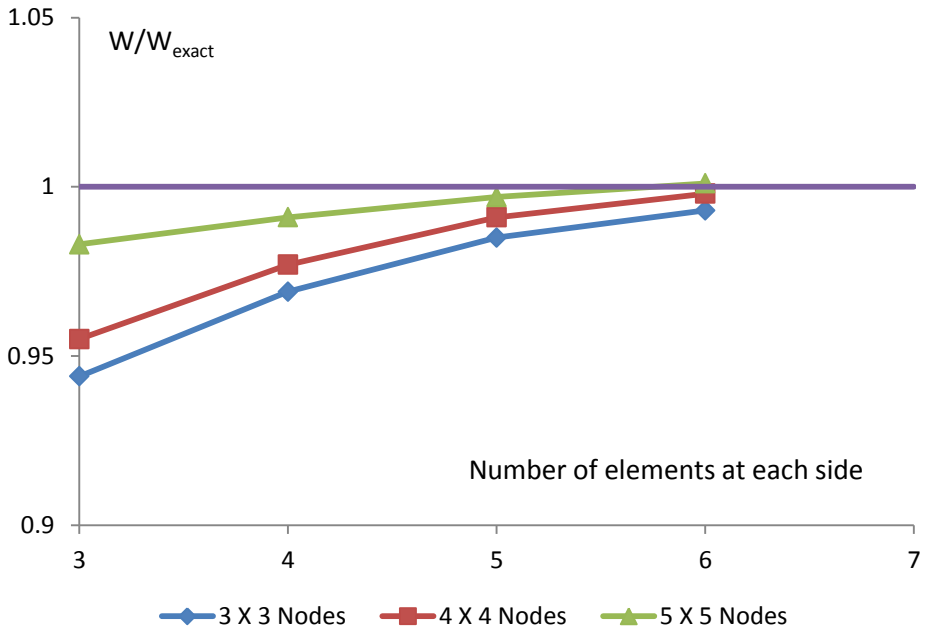


Figure 5.8: Convergence of different order shell elements

Table 5.3 provides the center deflections of the laminated plate under uniform load. The nonlinear behavior of this example is plotted in Figure 5.9. In Figure 5.9, the nonlinear behavior by J. N Reddy [20] is also plotted.

Table 5.3: Center deflections of laminated plate under uniform load

| $q_0$ ($psi$) | Deflection ($in$) |
|---|---|
| 100 | 0.1654 |
| 200 | 0.2275 |
| 400 | 0.3015 |
| 600 | 0.3510 |
| 800 | 0.3895 |
| 1000 | 0.4216 |
| 1200 | 0.4496 |
| 1400 | 0.4744 |
| 1600 | 0.4968 |
| 1800 | 0.5173 |

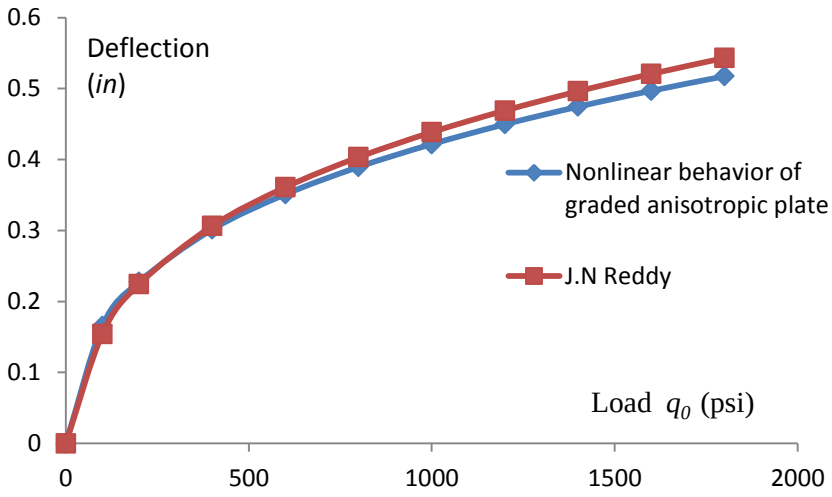


Figure 5.9: Nonlinear behavior of laminated plate

## 5.3 Material parameter grading for anisotropic materials

This example focuses on the material grading only by changing in parameters (not direction) for an anisotropic material.

It is necessary to introduce mechanical model for unidirectional fiber-reinforced materials. In J. N. Reddy [20], unidirectional fiber-reinforced materials are modeled as orthotropic material, with principal orientations parallel and transverse to the fiber directions.

The coordinate system $(x_1 - x_2 - x_3)$ is set up as shown in Figure 5.10, in which $x_1$ is chosen parallel to fiber direction. Here we assume the matrix and fiber are both isotropic materials, and they have the material parameters given by

$$E_f = Elasticity\ modulus\ of\ fiber; \qquad E_m = Elasticity\ modulus\ of\ matrix;$$

$$G_f = shear\ modulus\ of\ fiber; \qquad G_m = shear\ modulus\ of\ matrix$$

$\nu_f = Poisson's\ ratio\ of\ fiber;$ $\nu_m = Poisson's\ ratio\ of\ matrix;$

$V_f = Fiber\ volum\ fraction;$ $V_m = Matrix\ volum\ fraction.$

The material parameters for lamina with respect to principal orientations can be calculated as

$$E_1 = E_f\, V_f + E_m V_m, \qquad \nu_{12} = \nu_f V_f + \nu_m V_m,$$
$$E_2 = \frac{E_f E_m}{E_f\, V_m + E_m V_f}, \qquad G_{12} = \frac{G_f G_m}{G_f\, V_m + G_m V_f}. \tag{5.1}$$

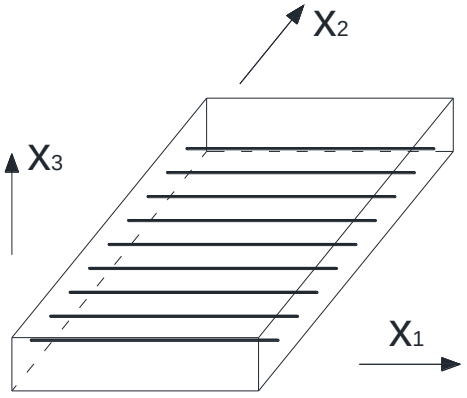


Figure 5.10: A unidirectional fiber-reinforced composite

A graded unidirectional fiber-reinforced square plate is considered with dimensions $a = b = 10\ inch$ for width and length, and $t = 1.0\ inch$ for the thickness. The plate is simply supported using the SS-1 boundary conditions that were used in example 1 and 2 in Chapter 4. A uniform distributed load $q_0$ is applied over the full surface of the plate.

The fiber and matrix have material parameters $E_f = 10^7\ psi, E_m = 10^6\ psi, \nu_f = \nu_m = 0.25$. The fiber volume fraction linearly changes from 10% at the bottom to 50% at the top, and it can be expressed as $\nu_f = 0.1 + 0.4x_3$, in which $x_3$ is the coordinate along thickness.

Material parameters for graded anisotropic plate can be calculated as

$E_1 = (1.9 + 3.6x_2) \times 10^6\ psi, E_2 = E_3 = \frac{10}{9.1-3.6x_2} \times 10^6\ psi, G_{12} = G_{13} = \frac{1.6}{3.64-1.46x_2} \times 10^6\ psi, G_{23} = 0.4 \times 10^6\ psi, \nu_{12} = \nu_{13} = \nu_{23} = 0.25.$

The convergence rates of different order elements are studied, and the results are shown in Figure 5.11. The FE model is meshed with up to $5 \times 5$ shell elements, each element having up to $5 \times 5$ nodes. The nonlinear results of graded fiber-reinforced plate are provided in Table 5.4. Linear and nonlinear behaviors are plotted in Figure 5.12 and 5.13.

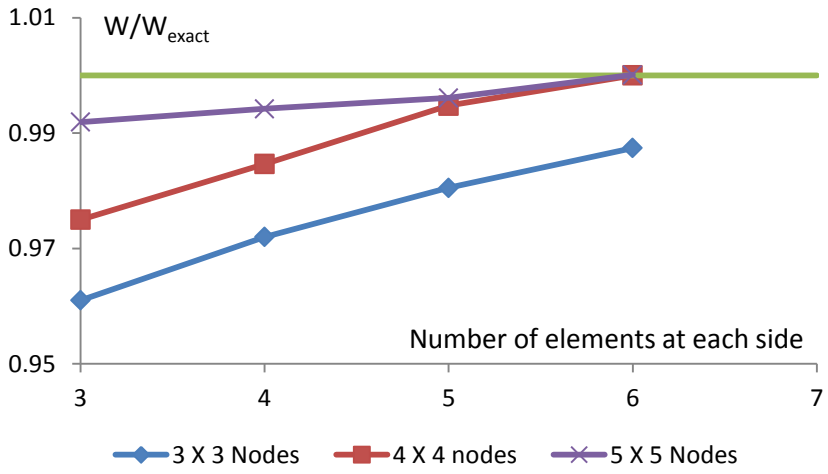


Figure 5.11: Convergence of different order elements

Table 5.4: Center deflections of graded fiber-reinforced plate under uniform load

| Load (*psi*) | Deflection (*in*) | Load (*psi*) | Deflection (*in*) |
|---|---|---|---|
| 400 | 0.100 | 3600 | 0.525 |
| 800 | 0.184 | 4000 | 0.557 |
| 1200 | 0.255 | 4400 | 0.586 |
| 1600 | 0.315 | 4800 | 0.613 |
| 2000 | 0.367 | 5200 | 0.639 |
| 2400 | 0.413 | 5600 | 0.664 |
| 2800 | 0.454 | 6000 | 0.687 |
| 3200 | 0.491 | 6400 | 0.709 |

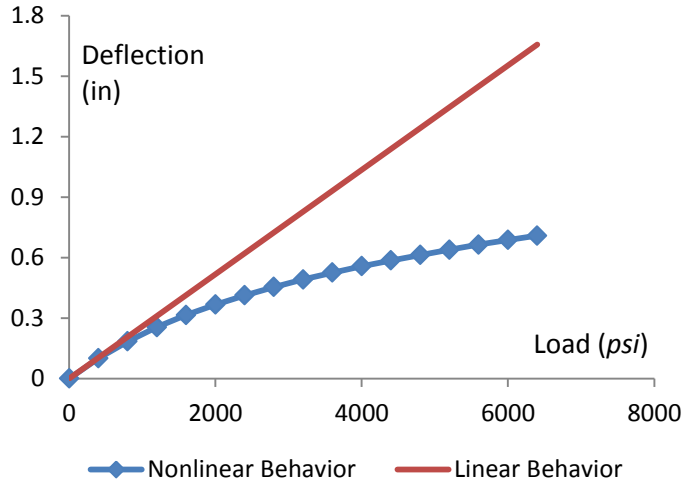


Figure 5.12: Linear and nonlinear behaviors for graded fiber-reinforced plate

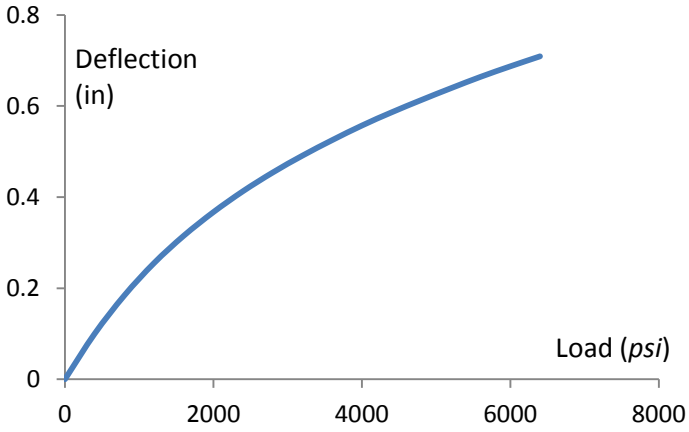


Figure 5.13: Nonlinear behaviors for graded fiber-reinforced plate

Consider the structure of Bamboo as shown in Figure 5.14 and 5.15. The composition of fibers varies along the radius of the bamboo. Bamboo and wood are naturally graded anisotropic materials with material parameters vary along radius of the cross-section. The method introduced in this example can also be used the FE analysis of bamboo and wood with isotropic properties that change.

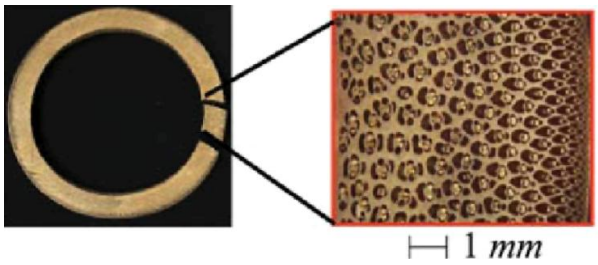


Figure 5.14: Fiber variations on cross-section of bamboo (E. C. Nelli Silva et al. [17])

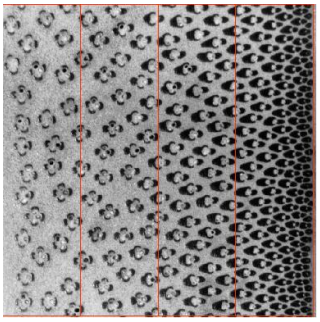

Figure 5.15: Fiber variations details (K. Ghavami et al. [24])

## 5.4 Composite reinforced by curved fibers

**Case 1:**

In this example a plate is reinforced by curved fibers as shown in Figure 5.16. The fibers follow the function $y = \frac{1}{25}(x^2 - 10x)$ as shown in Figure 5.17. The material parameters along the principal orientations, which are parallel and transverse to the fiber directions, are

$E_1 = 3.7 \times 10^6 psi, E_2 = E_3 = 1.37 \times 10^5\ psi, G_{12} = G_{13} = 0.55 \times 10^6\ psi, G_{23} = 0.4 \times 10^6\ psi, \nu_{12} = \nu_{13} = \nu_{23} = 0.25.$

Since the fibers are curved, the rotation angle $\theta$ of material orientations can be expressed as: $\theta = tan^{-1}(\frac{2x-10}{25})$ .

This plate has 10 $inch$ for width and length, and 1.0 $inch$ for thickness. The plate is simply supported at sides of b and d. A uniform load $q_0$ is applied over the full surface of the plate.

The convergence rates of different order elements are studied, and the results are shown in Figure 5.18. The FE model is meshed with up to $5 \times 5$ shell elements, each element having up to $5 \times 5$ nodes. Due to the effect of curved fibers, one can expect that the area around the center of c side can have larger normal stress and bigger transverse deflection than the rest part of plate. Those are shown in Figure 5.19 and Figure 5.20.

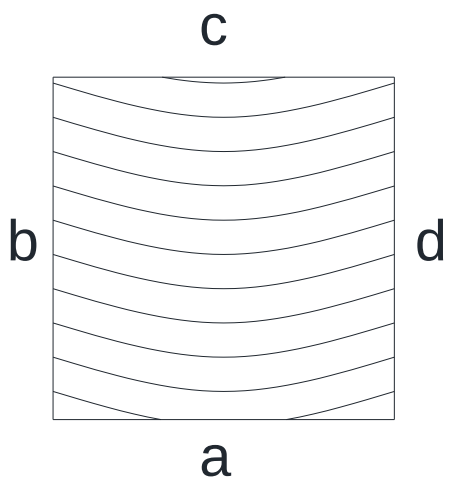


Figure 5.16: Top view of plate reinforced by curved fibers

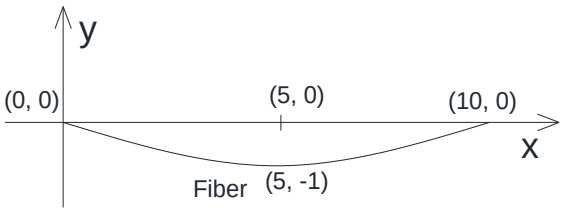


Figure 5.17: Shape of fibers

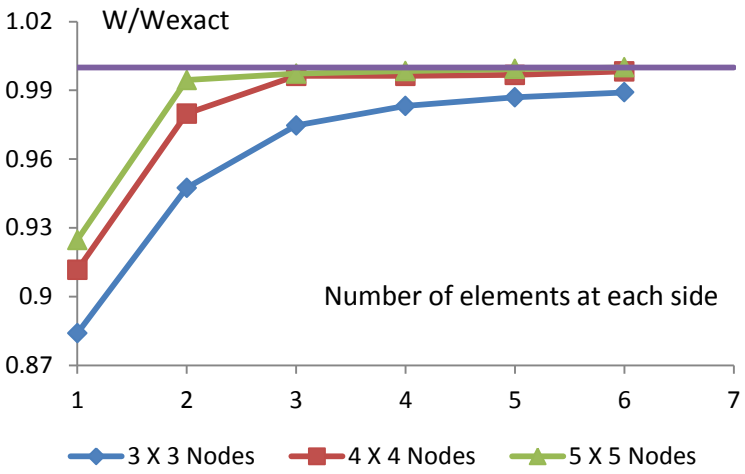


Figure 5.18: Convergence of different order elements

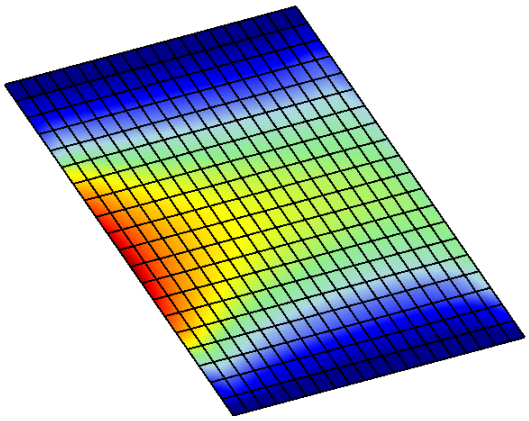

Figure 5.19: Longitudinal stress distribution of plate

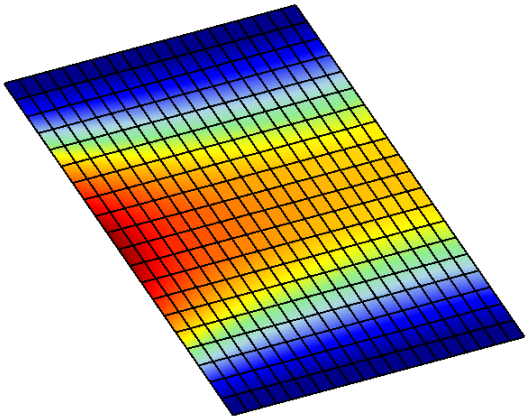

Figure 5.20: Transverse deflection of plate

The geometrically nonlinear behaviors of plate are studied in this example. The deflections at the center of sides of a and c are provided in Table 5.5. The center deflections of a and c sides are plotted in Figure 5.21. As shown in this Figure, difference of two groups of deflections increases as uniform load increases. The deformed shape of plate is shown in Figure 5.22.

Table 5.5: The center deflections of sides of a and c

| Load ($psi$) | Center deflections of $c$ side ($in$) | Center deflections of $a$ side ($in$) |
|---|---|---|
| 500 | 0.295 | 0.206 |
| 1000 | 0.578 | 0.408 |
| 1500 | 0.842 | 0.602 |
| 2000 | 1.086 | 0.789 |
| 2500 | 1.311 | 0.967 |
| 3000 | 1.517 | 1.136 |
| 3500 | 1.707 | 1.296 |
| 4000 | 1.880 | 1.447 |

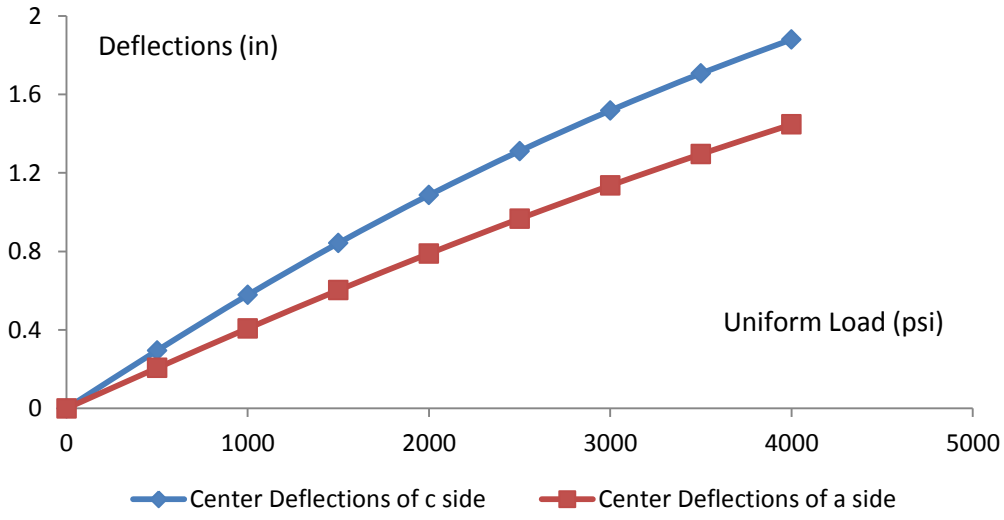


Figure 5.21: Center transverse deflections of a and c sides

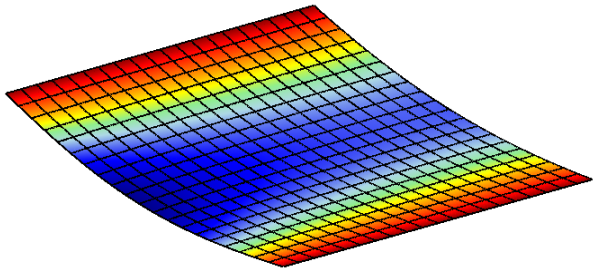

Figure 5.22: Deformed shape of fiber reinforced plate

**Case 2:**

In this case, a cantilever has l0 inch for length, 1 inch for thickness and width. The cantilever is reinforced by circular fibers as shown in Figure 5.23. The radii of fibers are chosen as 8 in, 13 in, 18 in, 23 in, and 30 in, respective. This cantilever has one uniform vertical force at its free end; three uniformly distributed load steps are chosen as 200 lb/in, 400 lb/in, and 600 lb/in, respectively. Given that material parameters of cantilever on principle orientations are: $E_1 = 3.7 \times 10^6 psi, E_2 = E_3 = 1.37 \times 10^5\ psi, G_{12} = G_{13} = 0.55 \times 10^6\ psi, G_{23} = 0.4 \times 10^6\ psi, \nu_{12} = \nu_{13} = \nu_{23} = 0.25.$

Since the fibers are curved, the rotation angle $\theta$ of material orientations can be expressed as: $\theta = tan^{-1}(\frac{x-5}{\sqrt{\rho^2-(x-5)^2}})$ .

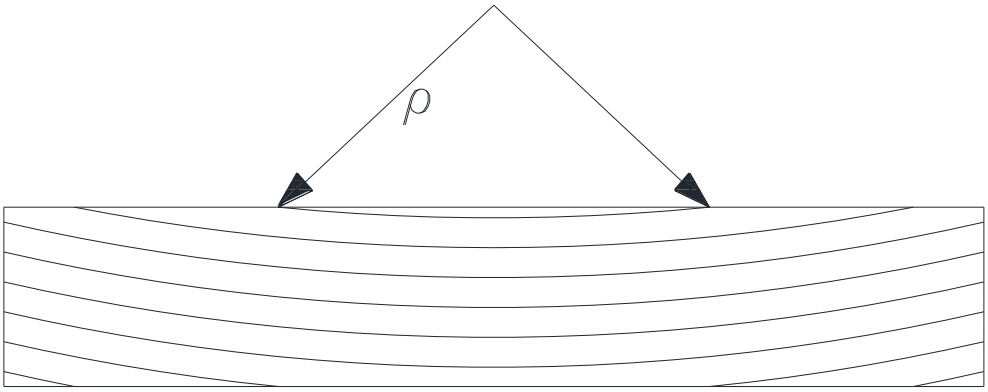


Figure 5.23: Cantilever reinforced by circular fibers with radius $\rho$

In this case, due to the effect of circular fibers, one can expect that there will be rotation angles at the free end of cantilever. At each load level, the transverse deflections of the most left tip and the most right tip at the free end of cantilever are obtained in FEA. Since rotation angle is small, it can be simply calculated from transverse deflection of those two tips dividing by width of cantilever, and that is $\varphi = \frac{\delta_l - \delta_r}{1} = \delta_l - \delta_r$. The rotation angles at the free end of cantilever with respect to each load level are provided in Table 5.5.

Table 5.6: Rotation angles at the free end of cantilever

| Uniform Load (lb/in) | Fiber Radius: 8 in | Fiber Radius: 13 in | Fiber Radius: 18 in | Fiber Radius: 23 in | Fiber Radius: 30 in |
|---|---|---|---|---|---|
| | Rotation Angle ($rad^{-3}$) | | | | |
| 200 | 8.501 | 6.713 | 5.139 | 4.113 | 3.196 |
| 400 | 16.913 | 13.383 | 10.251 | 8.205 | 6.378 |
| 600 | 25.153 | 19.968 | 15.309 | 12.258 | 9.530 |

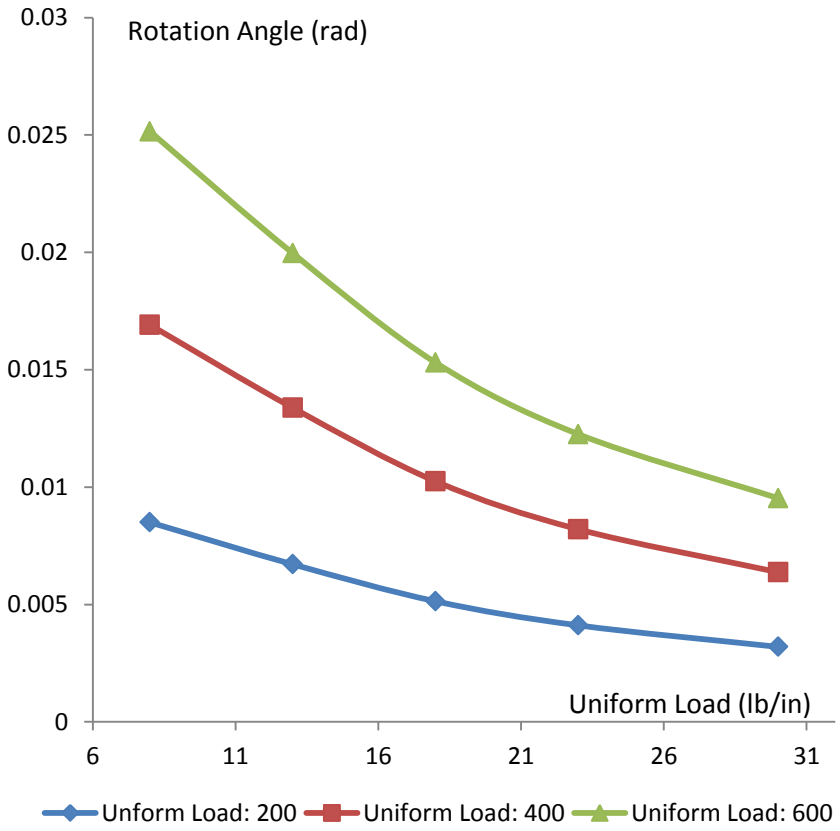


Figure 5.24: Cantilever reinforced by circular fibers with radius

## 5.5 Woven material

In this example, a plate is reinforced by five fibers and details are shown in Figure 5.25, 5.26, 5.27 and 5.28.

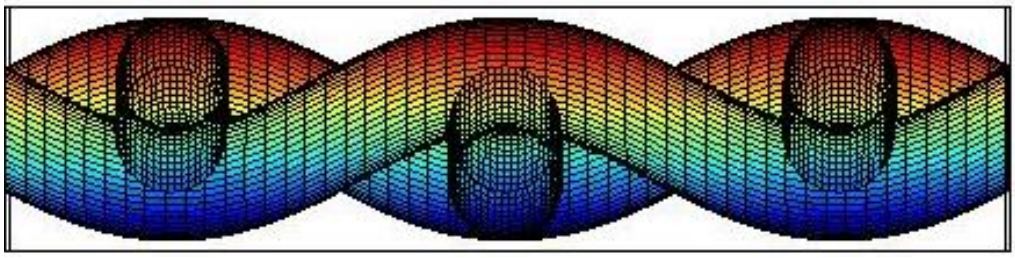

Figure 5.25: Front view of woven material plate

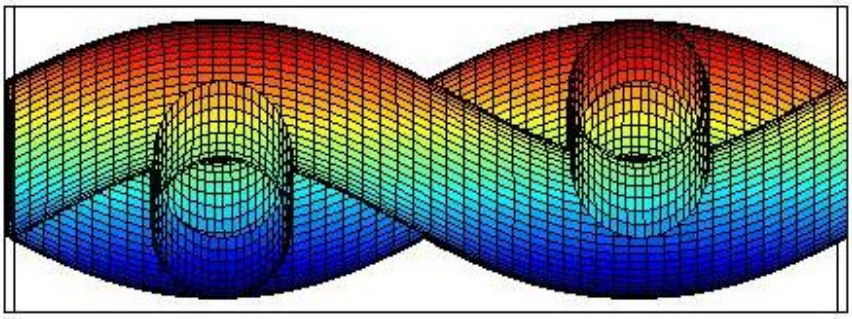

Figure 5.26: Side view of woven material plate

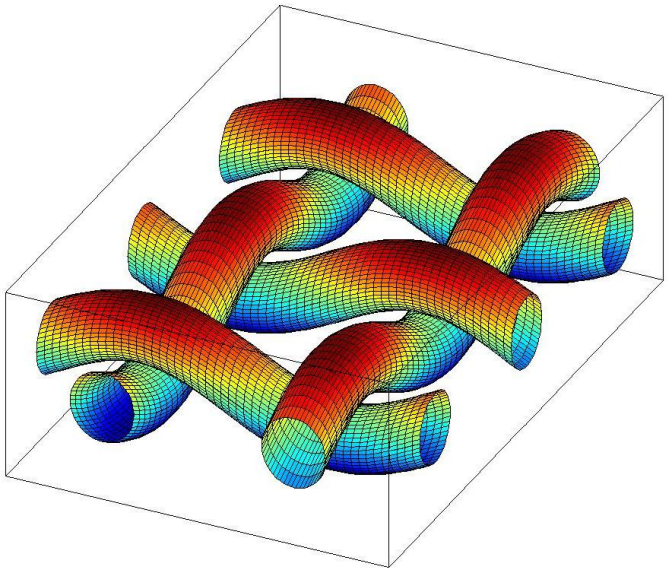

Figure 5.27: Details of woven material plate (1)

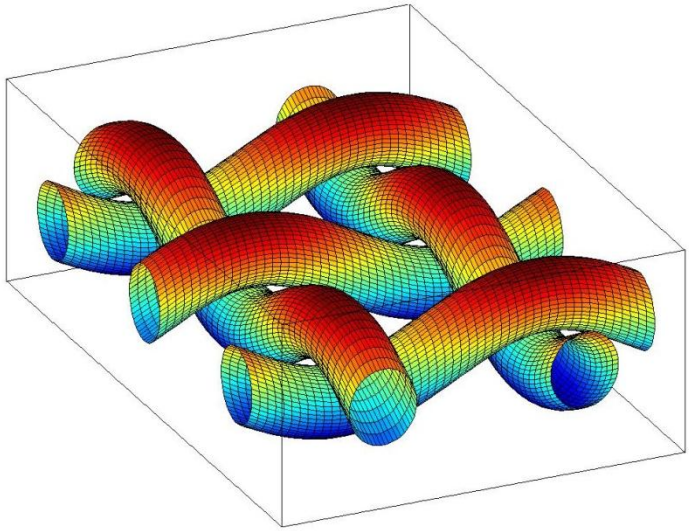

Figure 5.28: Details of woven material plate (2)

As shown in the above figures, five fibers travel up and down in plate and interweave with each other. The centerlines of fibers can be expressed as:

Fiber 1: $$\begin{cases} y = 3 \\ z = \sin\left(\frac{\pi x}{6}\right) + 2.2 \end{cases} \quad (5.2)$$

Fiber 2: $$\begin{cases} y = 9 \\ z = \sin(\frac{\pi x}{6} + \pi) + 2.2 \end{cases} \quad (5.3)$$

Fiber 3: $$\begin{cases} y = 15 \\ z = \sin(\frac{\pi x}{6}) + 2.2 \end{cases} \quad (5.3)$$

Fiber 4: $$\begin{cases} x = 3 \\ z = \sin(\frac{\pi y}{6} + \pi) + 2.2 \end{cases} \quad (5.4)$$

Fiber 5: $$\begin{cases} x = 9 \\ z = \sin(\frac{\pi y}{6}) + 2.2 \end{cases} \quad (5.5)$$

The matrix has material properties: elastic modulus $E = 1000\,psi$, and Poisson's ratio $\nu = 0.3$. And the fibers have material properties: $E = 1000\,psi$, and $\nu = 0.3$. The fibers have radii of 1 inch. The plate makes a cantilever, and the cantilever has 4.4inch for its thickness, 12 inch for its length, and 18 in for its width. The cantilever is loaded with an axial force at its free end. As a matter of convenience, surface a denotes the surface that has three fibers on it, and surface b denotes the surface has two fibers on it. One can tell surface a has an axial force on it in the cantilever.

In traditional FEA, this plate has to be meshed into thousands of elements in order to analyze its behavior. Since the function driven strategy is robust in capturing material grading in the body, this plate can be analyzed with much less elements. In this example, with function driven strategy, only one high order brick element is used to simulate the plate's behaviors. This element has $6 \times 6 \times 6$ nodes, and $9 \times 9 \times 9$ integration points.

Normal strain distribution on longitudinal direction for plate is shown in Figure 5.29. As can be seen from this Figure, three regions of strain concentration are on the free-end cross section. Two regions of strain concentration can also be seen from the other side in Figure 5.30.

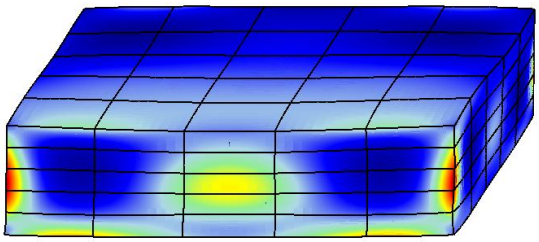

Figure 5.29: Normal strain distribution on longitudinal direction on surface a

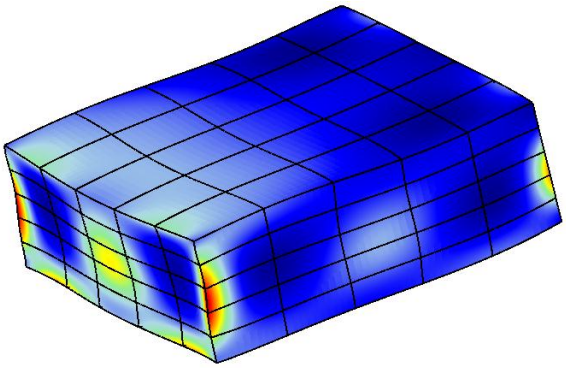

Figure 5.30: Normal strain distribution on longitudinal direction on surface b

Under axial load, the fibers try to straighten. As the fibers straighten, they drag down or pull up the material of neighborhood. Therefore, one can expect that there is transverse deflection for this cantilever. And the transverse deflection of cantilever is shown in Figure 5.31. Under uniform load of 100 psi, the cantilever has the maximum transverse deflection of 0.341 in.

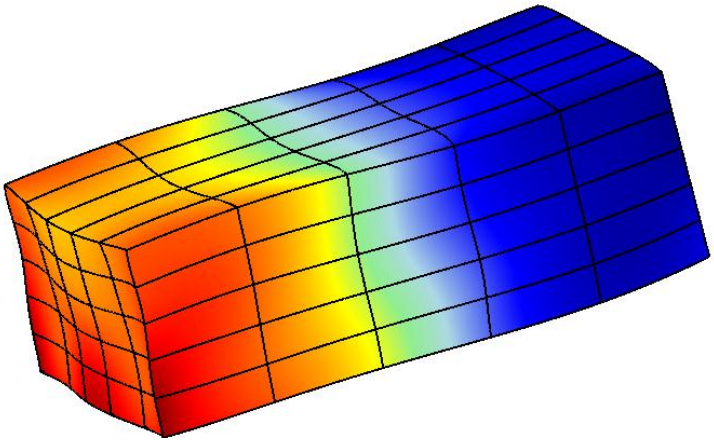

Figure 5.31: Transverse deflection of cantilever

Since fibers have higher elastic moduli than matrix, they try to pull back the material of neighborhood in the extension. Therefore, the plate cannot evenly extend. As can be seen in Figure 5.32, the free-end cross section actually bumps in and out. The maximum extensions happen at the corners of cross section, and the minimum extensions happen at the midpoints of two side fibers.

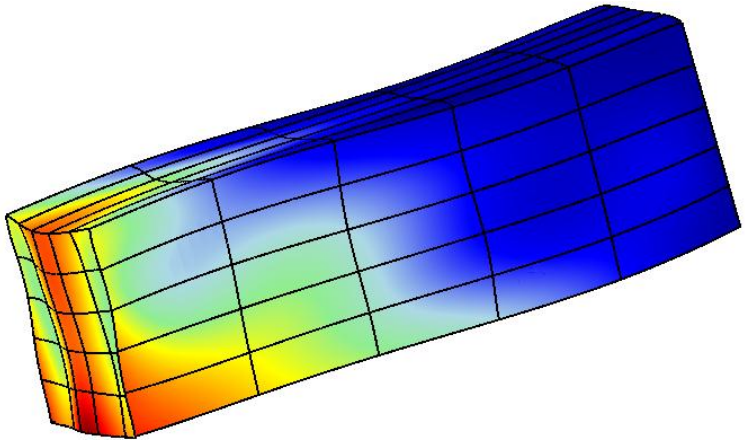

Figure 5.32: Extension of cantilever

Let's look at the summit part of middle fiber. As the middle fiber straightens, this part goes down, and pulls down the material around it. By doing so, it creates a bending effect in a local volume. As shown in Figure 5.33, the region on the top of cantilever that is close to the middle fiber summit has a compressive stress concentration. One can also find another two major regions and three minor regions of compressive stress concentration in Figure 5.33.

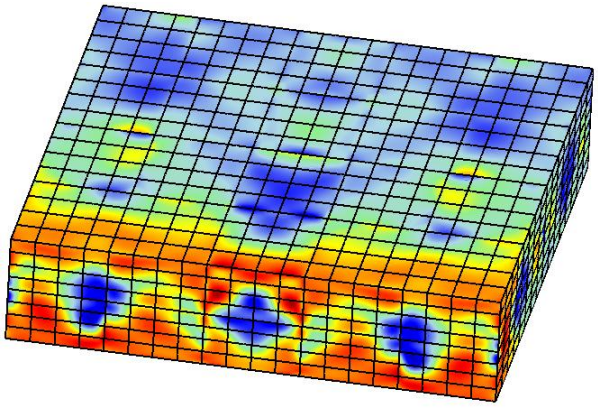

Figure 5.33: Longitudinal stress of plate

## 5.6 Conclusion

This chapter analyzed the geometrically linear and nonlinear behaviors of several graded material problems. The first example studies the linear and nonlinear behaviors of an isotropic plate with material grading in the thickness. Different from regular plate, this graded plate can have transverse deflection under axial force. However, the transverse deflection of plate can eventually reach a limit due to the second order effect. The second example is to study the behaviors of a laminated composite, which is a typical case for anisotropic material with orientation grading. The third example introduced a method to generalized fiber-reinforced material, and used this method to study the behavior of anisotropic materials with material parameter grading. Since bamboo and wood also have similar material grading to this example, the method in this example can also be used the FE analysis of bamboo and wood. The fourth example tried to analyze a more complex fiber-reinforced material, that the fibers are curved in matrix. The fifth example tries to use on high order brick element to study the behaviors of complicated woven material plate. To sum up, this chapter used several examples to explore the possibility to apply the strategies and constitutive model to graded materials.

# Chapter 6 Conclusions

This thesis looks at generic strategies for the finite element method implementation for graded materials. In order to achieve this goal, three generic strategies are proposed to transfer material grading into the finite element solution, and a constitutive model is developed to deal with material grading in isotropic and anisotropic materials and implemented into the finite element formulation.

The strategies proposed in this thesis are a global node-driven strategy, an element driven strategy, and a function-driven strategy.

For the global node driven strategy and the element driven strategy, the finite element solver obtains the material grading at each integration point through interpolation of nodal properties. The difference between the global node driven and the element driven strategies are compared in details in Chapter 3. In general, the global node driven strategy requires the finite element model to carry less material grading information than the element driven strategy. The element driven strategy can better model discontinues jumps in the values of properties than the global node driven strategy can. However, if the material properties are gradually graded, both strategies generate identical results.

For the function driven strategy, the finite element solver can obtain the properties through visiting material grading functions outside of the FE model. Compared to the other two strategies, the function driven strategy requires minimal additional memory to store grading in the materials. In the cases of gradual grading, the function driven strategy provides very close results to other two strategies. In the cases of material property jumps, the function driven strategy yields accurate results with less elements or lower order elements. If there is material

grading in the thickness, the function driven strategy is more convenient than the other two strategies for the shell formulation. Detailed comparisons among strategies can be found in Chapter 3.

A constitutive model that considers large deformation of material is developed in order to deal with material grading. This model is applicable to both isotropic and anisotropic materials. The material grading, either in the form of parameters or orientations, can be expressed by variations of the elasticity tensor of the material. This model is verified through two examples. One is an isotropic plate and the another is and orthotropic plate. Details of the constitutive model can be found in Chapter 4.

By using the proposed strategies and the constitutive model, geometrical linear and nonlinear behaviors of several graded problems are studied. Among these examples, one example studies an isotropic plate/beam with material grading in the thickness. Due to the material grading, a cantilever made from this beam can also show transverse deflection under axial force, and this deflection will reach its limit due to second order nonlinear effect. The second example shows the finite element implementation for material parameter grading. The third example in Chapter 5 introduces a method to analyze fiber-reinforced material. The method of this example can also be used in FE analysis for naturally graded materials, for example bamboo. This method is used to demonstrate the behaviors of a composite reinforced by curved fibers, and both plate and beam examples are studied. Finally, we use the function driven method to define a woven fiber microstructure in a plate made of a resin and fiber. We use this example to demonstrate the separation of the function driven method from the FEM model. To do this we use only one element to solve the problem and show we can characterize the details of the microstructure.

Through verifications and comparisons, the strategies proposed in this thesis show obvious advantages to traditional FEM in transferring material grading into finite element soltion process. The constitutive model in this thesis is powerful in many kinds of material grading. By combining these strategies and nonlinear constitutive model, the finite element method can be more flexible in solving problems with complex material grading.

**Future work**

One can look at many different aspects of material grading both in specific examples and strategies to implement them. Two immediate areas that one may consider are:

1. Implementation of the function driven strategy in generic finite element programs that provide user defined subroutines for material implementation. The function driven strategy totally independent of the finite element model so one can implement it in any FEM solver that provides for user defined materials.
2. The proposed strategies can be all implemented to consider different material properties, such as heat conduction or electrical characteristics.

# Reference

[1] S. Pradyuma, Namita Nanda (2010). Geometrically Nonlinear transient analysis of functionally graded shell panels using a higher-order finite element formulation. Journal of mechanical engineering Research Vol. 2(2), pp. 39-51

[2] R. Naghadabadi, S. A. Hosseini Kordkheili (2005). A finite element formulation for analysis of functionally graded plates and shells. Archive of Applied Mechanics 74: 375-386

[3] G. N. Praveen, J. N. Reddy (1998). Nonlinear Transient thermoelastic analysis of FG ceramic-metal plates. Int J Solids Structure 35: 4457-4476

[4] G. N. Praveen, C. D. Chin, J. N. Reddy (1999). Thermoelastic analysis of FG ceramic-metal cylinder. J Eng Mech 125: 1259-1267

[5] J. N. Reddy (2000). Analysis of FG plates. Int J Number Meth Eng 47: 663-684

[6] N. El-Abbasi, S.A. Meguid (2000). Finite element modeling of the thermoelastic behavior of FG plates and shells. Int J Comput Eng Sci 1: 151 – 165

[7] L. D. Croce, P. Venini (2004). Finite elements for functionally graded reissner-mindlin plates. Comput methods Appl Mech Eng 193 (2004) 705 – 725

[8] Ki-Du Kim, G. R. Lomboy, Sung-Cheon Han (2008). Geometrically Non-linear Analysis of Functionally Graded material Plates and Shells using a Four-node Quasi-Conforming Shell Element. Journal of Composite Materials Vol. 42, No. 5

[9] M. Braun, M. Bischoff, E. Ramm (1994). Nonlinear Shell formulations for complete three-dimensional constitutive laws including composites and laminates. Computational Mechanics 15: 1-18

[10] R. A. Arciniega, J. N. Reddy (2006). Tensor-based finite element formulation for geometrically nonlinear analysis of shell structures. Comput. Mehods Appl. Mech. Engrg. 196: 1048 – 1073

[11] Mohamed Balah, Hamdan N. Al-Ghamedy (2002). Finite element formulation of a third order laminated finite rotation shell element. Computers & Structures.

[12] Dvorkin EN, Bathe KJ (1984). A continuum mechanics based on four-node shell element for general nonlinear analysis. Engng Comput 1: 77-88

[13] S. J. Lee, J. N. Reddy, F. Rostam-Abadi (2006). Nonlinear finite element analysis of laminated composite shells with actuating layers. Finite Elements in Analysis and Design. 43: 1-21

[14] W.T. Koiter, On the nonlinear theory of thin elastic shells, in: Proceedings Koninklijke Nederlandse Akademie vanWetenschappen, vol. B69,Amsterdam, 1996, pp. 1–54.

[15] J.N. Reddy, An Introduction to Nonlinear Finite Element Analysis, Oxford University Press, Oxford, UK, 2004.

[16] J.L. Sanders Jr., Nonlinear theories for thin shells, Quart. Appl. Math. 21 (1963) 21–36.

[17] E. C. Nelli Silva, Matthew C. Walters, Glaucio H. Paulino (2006). Modeling bamboo as a functionally graded material: lessons for the analysis of affordable materials. J Mater Sci 41: 6991-7004

[18] C.F. Liu, J.N. Reddy (1985). A higher-order shear deformation theory of laminated elastic shells, Int. J. Eng. Sci. 23 (3): 319–330.

[19] L. Vu-Quoc, X. G. Tan (2003). Optimal solid shells for non-linear analysis of multilayer composites. I. Statics. Comput. Methods Appl. Mech. Engrg. 192: 975-1016

[20] J. N. Reddy (2004).Mechanics of laminated composite plates and shells ------ Theory and Analysis, second edition, CRC press: 86-88

[21] T. Tan etc. (2011). Mechanical properties of functionally graded hierarchical bamboo structures. Acta Biomaterialia. Article in process.

[22] Shigeyasu Amada etc. (1997). Fiber texture and mechanical graded structure of bamboo. Composites part B 28B: 13-20

[23] K. Ghavami, C. S. Rodrigues and S. Paciornik (2003). Bamboo: Functionally Graded Composite Material. ASIAN JOURNAL OF CIVIL ENGINEERING (BUILDING AND HOUSING) VOL. 4, NO. 1, 1-10

[24] Mehrdad Negahban (March, 2012). The Mechanical and Thermodynamical Theory of Plasticity. CRC Press, Taylor & Francis Group

# Appendix

**Calculation for example 2 in Chapter 3**

The calculation steps based on beam theory for example 2.2 in chapter 2 are shown in this section. This example is detailed in chapter 3; figure below shows diagrams of cantilever, elasticity modulus, and bending moment.

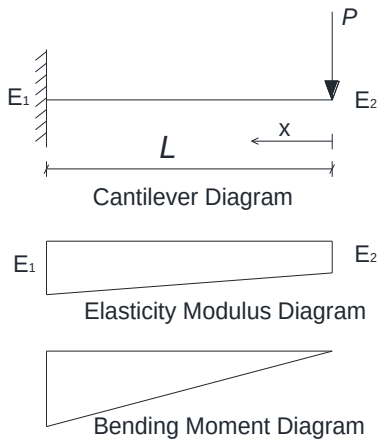


Figure A.1.1: Diagrams of cantilever, elastic modulus, and bending moment

Define two constants a and b as:

$$a = E2 \tag{A.1.1}$$

$$b = \frac{E1 - E2}{E2 \times L} \tag{A.1.2}$$

Express elastic modulus as function of position:

$$E(x) = a(1 + bx) \tag{A.1.3}$$

Set up relation between deflection and bending moment according to beam theory:

$$EIv'' = M \text{ (A.1.4)} \qquad \text{(A.1.4)}$$

Express bending moment and second derivative of deflection as functions of positions:

$$M(x) = Px \qquad \text{(A.1.5)}$$

$$v''(x) = \frac{M(x)}{E(x)I} = \frac{p}{abI}\left(1 - \frac{\frac{1}{b}}{x + \frac{1}{b}}\right) \qquad \text{(A.1.6)}$$

Build boundary conditions for cantilever:

B.C. 1: $$v'(x = L) = 0 \qquad \text{(A.1.7)}$$

B.C. 2: $$v(x = L) = 0 \qquad \text{(A.1.8)}$$

Obtain deflection function by using boundary conditions:

$$v = \frac{p}{abI}\left[\frac{x^2}{2} - \frac{x}{b}\ln\left(x + \frac{1}{b}\right) - \frac{1}{b^2}\ln\left(x + \frac{1}{b}\right) + \frac{x}{b} + \frac{x}{b}\ln\left(L + \frac{1}{b}\right) - Lx + \frac{L^2}{2} + \frac{1}{b^2}\ln\left(L + \frac{1}{b}\right) - \frac{L}{b}\right] \qquad \text{(A.1.9)}$$

Obtain maximum deflection of cantilever (at free end)

$$v_{max} = v(x = 0) = \frac{p}{abI}\left[-\frac{1}{b^2}\ln\frac{1}{b} + \frac{L^2}{2} + \frac{1}{b^2}\ln\left(L + \frac{1}{b}\right) - \frac{L}{b}\right] \qquad \text{(A.1.10)}$$

Therefore, plug constants into equation A.1.10 to get the relation between maximum deflection and loading:

$$v_{max} = 3.6558p \qquad \text{(A.1.11)}$$

**Appendix 1.2 Calculation for example 3 in Chapter 3**

The calculation steps based on beam theory for example 3 in Chapter 3 are shown in this section. This example is detailed in Chapter 3; Figure A.1.2 and A.1.3 below show diagrams of cantilever, elasticity modulus, and bending moment.

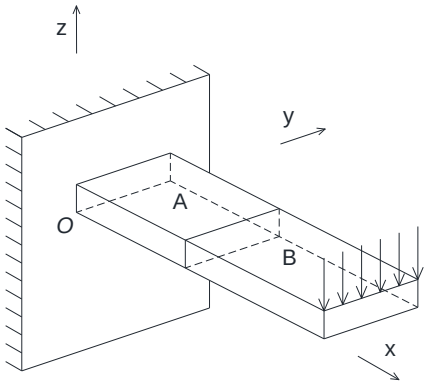


Figure A.1.2: Cantilever diagram

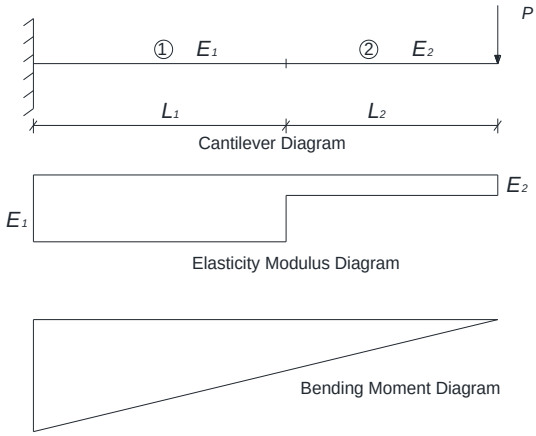


Figure A.1.3: Diagrams of cantilever, elastic modulus, and bending moment

Express bending moment as function of force and position:

$$M(x) = pl - px \tag{A.1.12}$$

Set up relation between deflection and bending moment according to beam theory:

$$EIv'' = M(x) \tag{A.1.13}$$

Modify Equation A.1.13 due to difference of materials along length:

$$\begin{cases} E_1 I v_1'' = M(x) \\ E_2 I v_2'' = M(x) \end{cases} \tag{A.1.14}$$

Two second order derivate equations of deflection will generate four unknowns, which will need four boundary conditions to solve problem. And due to geometric continuity, two extra conditions can be built at the boundary between two parts besides the two boundary conditions that cantilever usually has at their fixed end. And the boundary conditions are given:

$$\begin{cases} v_1'(x = 0) = 0 \\ v_1(x = 0) = 0 \\ v_1'(x = l_1) = v_2'(x = l_1) \\ v_1(x = l_1) = v_2(x = l_1) \end{cases} \tag{A.1.15}$$

Solve the differential equations of deflections to obtain results as follows:

$$\begin{cases} v_1 = \dfrac{6px^2 - px^3/6}{E_1 I} \\ v_2 = \dfrac{6px^2 - \dfrac{px^3}{6} - 40.5px + 108p}{E_2 I} \end{cases} \tag{A.1.16}$$

And the maximum deflection (at the free end of cantilever) is equal to $4.752\mathrm{p}$.

**Appendix 1.3 Calculation for example 1 in Chapter 5**

Figure A.1.4 and A.1.5 are separately diagrams of elastic modulus variation along thickness, and horizontal loading at the cantilever.

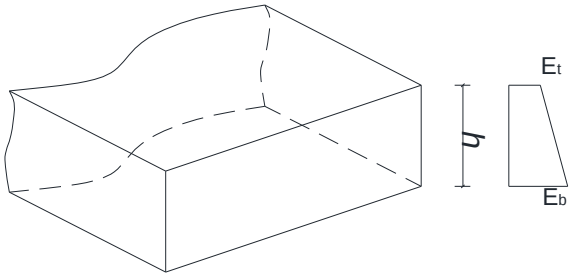


Figure A.1.4: Elastic modulus variation along thickness

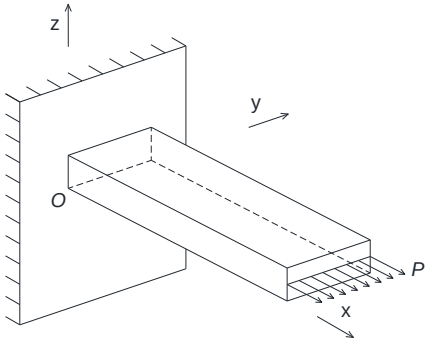


Figure A.1.5: Horizontal loading at the free end of cantilever

Assume cross-section of the cantilever remain plane during bending, and assume the plane curvature for a cross section is $\emptyset$, diagrams of strain and stress along thickness of cantilever are shown in Figure A.1.6

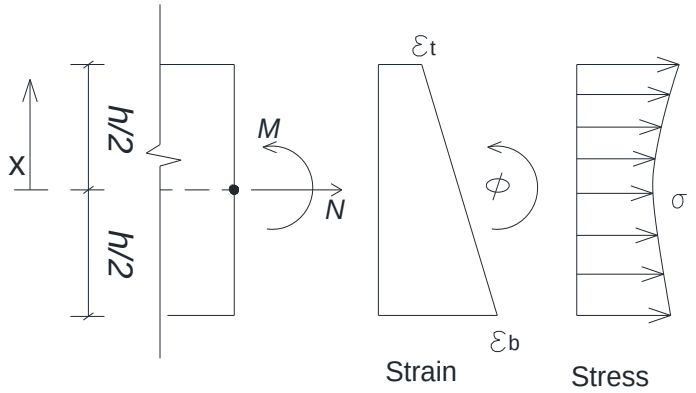


Figure A.1.6: Strain and stress diagram along thickness of cantilever

Elastic modulus:

$$E(x) = E_t\left(\frac{x}{h} + \frac{1}{2}\right) - E_b(\frac{x}{h} - \frac{1}{2}) \tag{A.1.17}$$

Strain along thickness:

$$\varepsilon(x) = \varepsilon_t\left(\frac{x}{h} + \frac{1}{2}\right) - \varepsilon_b(\frac{x}{h} - \frac{1}{2}) \tag{A.1.18}$$

Axial force on the cross-section:

$$N = b\int_{-\frac{h}{2}}^{\frac{h}{2}} E(x)\varepsilon(x)dx = \frac{bh}{6}(2E_b\varepsilon_b + 2E_t\varepsilon_t + E_b\varepsilon_t + E_t\varepsilon_b) \tag{A.1.19}$$

Bending moment on the cross section:

$$N = b\int_{-\frac{h}{2}}^{\frac{h}{2}} E(x)\varepsilon(x)dx = \frac{bh}{6}(2E_b\varepsilon_b + 2E_t\varepsilon_t + E_b\varepsilon_t + E_t\varepsilon_b) \tag{A.1.20}$$

Bending curvature on the cross section:

$$\phi = (\varepsilon_b - \varepsilon_t)/h \tag{A.1.21}$$

A horizontal loading is applied at the free end of cantilever. Since there is no bending moment applied onto cantilever, bending moment at any cross section should be equal to zero, which is M =0.

Therefore, the relations between top strain and bottom strain are:

$$\varepsilon_t = \frac{E_b}{E_t}\varepsilon_b \tag{A.1.22}$$

And one can obtain the bending curvature at cross section:

$$\phi = \frac{\varepsilon_b - \varepsilon_t}{h} = \frac{E_t - E_b}{E_t} \times \frac{\varepsilon_b}{h} \quad \text{(A.1.23)}$$

Given an axial force, one can straightforwardly calculate a constant curvature corresponding to that axial force. Since axial force is constant, bending curvature is constant along the entire cantilever. Therefore, although there is no bending moment applied onto it, this cantilever deforms exactly like a cantilever under a bending moment applied at its free end.

Therefore, one can get deflection of cantilever:

$$v(x) = \frac{1}{\phi} - \sqrt{(\frac{1}{\phi})^2 - x^2} \quad \text{(A.1.24)}$$

And the deflection at free end:

$$\delta = 0.023077P. \quad \text{(A.1.25)}$$